MODEL CORRELATION STUDY OF A RETRACTABLE BOOM FOR A SOLAR SAIL SPACECRAFT

O. Adetona and L.H. Keel
Tennessee State University
Nashville, Tennessee

J.D. Oakley, K. Kappus, M.S. Whorton, Y.K. Kim, and J.M. Rakoczy
NASA Marshall Space Flight Center
Huntsville, Alabama

ABSTRACT

To realize design concepts, predict dynamic behavior and develop appropriate control strategies for high performance operation of a solar-sail spacecraft, we developed a simple analytical model that represents dynamic behavior of spacecraft with various sizes. Since motion of the vehicle is dominated by retractable booms that support the structure, our study concentrates on developing and validating a dynamic model of a long retractable boom. Extensive tests with various configurations were conducted for the 30 Meter, light-weight, retractable, lattice boom at NASA MSFC that is structurally and dynamically similar to those of a solar-sail spacecraft currently under construction. Experimental data were then compared with the corresponding response of the analytical model. Though mixed results were obtained, the analytical model emulates several key characteristics of the boom. The paper concludes with a detailed discussion of issues observed during the study.

INTRODUCTION

Solar sails offer a safe, cost effective and propellant free mode of space transportation. These spacecraft are propelled by momentum gained when photons are absorbed and/or reflected from its large membranes. Ideally these membranes should be perfectly flat, to maximize thrust magnitude and optimize thrust vector control. For square solar sails, long light-weight coilable booms are needed to support the tensioned membranes in the same way long thin rods support a kite's fabric. Due to their light weight and long length, these booms will be highly flexible and lightly damped. When disturbed, they will respond with large amplitude slowly decaying vibration. This will lead to a loss of membrane flatness and deterioration of overall performance of the space vehicle. To realize the design concepts, predict dynamic behavior of the system and develop appropriate control strategies for high performance operation of the vehicle, accurate analytical models and model parameters are required. Therefore, the primary question we ask in this study is: can the dynamic behavior of an extremely large, typically 100 Meter by 100 Meter, square, solar-sail spacecraft be predicted by a standard linear scalable mathematical model? Since we expect vehicle motion will be dominated by dynamics of its booms, we limit our study to boom dynamics only.

It is known that lattice booms are well suited to providing structural strength to a solar-sail spacecraft for several reasons. Some of these reasons are: (1) their high strength-to-weight and length-to-diameter ratios, and (2) their ability to collapse to a small length/volume and subsequently deploy to much larger lengths/volumes. These durable, lightweight, open lattice structures can be retracted (by elastically coiling longerons to assume a flattened, helical configuration) into storage volumes with lengths of about 2% of deployed length. Once retracted they are easily stored/transported. Furthermore, availability of an ultra-lightweight space deployable 30 Meter boom at MSFC with structural properties of booms that can be used for solar-sail spacecraft enables us to perform this study.

Approved for public release, distribution is unlimited.
Portions of this effort were performed under grant number NNM05AA13G with the NASA Marshall Space Flight Center.

Mathematical models representing its static and dynamic characteristic behavior are derived and validated using experimental data from a 30 Meter long ABLE boom. The boom will operate in a zero gravity environment but tests will be performed in a one-g environment. Accordingly, the analytical models explicitly account for gravity in a manner that allows us to validate the model in a one-g environment and subsequently derive a zero-g model. Though model validation results were mixed, our results generally suggest that simple analytical models can account for the static and dynamic behavior of ABLE Lattice booms at long lengths.

The paper is organized as follows. In the *specifications of the boom* section, the boom description, dimensions and properties are discussed. This is followed by the *experimental setup* section which describes tests and test configuration. The *beam parameters* section provides parameters required to complete the analytical models. Due to the significance of bending stiffness and a variety of issues associated with it, the *bending stiffness determination* section is provided next. This is followed by the *mathematical models* section that contains models for bending and torsion along with all necessary assumptions. In the *data analysis* section, analysis obtained from comparing the response of models with experimental data is given. The paper is concluded with a *discussion* section and some remarks.

EXPERIMENTAL SETUP

The boom that was tested is a canister deployed boom capable of fully automatic deployment/retraction. Canister deployed booms are motor-driven, and the boom is extruded from an internally-threaded canister shell. A beneficial feature of these booms is the fact that near full stiffness and strength is achieved throughout the deployment phase[1,11]. The tested Mast/Canister system is a canister deployed boom that has been flown aboard the challenger space shuttle and subsequently deployed in space in 1984. Afterwards, it was modified for CASES ground tests[4].

As in Figure 1, the free end of the beam has a stiffener section (tip-bars) and the tip ring was removed for bending tests. However, the Tip-Ring was reinstalled to apply torsional forces for torsional tests. At the center of the tip-ring assembly is a bearing that prevents transverse motion in x and y directions but permits z axis rotary motion. The resulting arrangement for torsional tests is illustrated in Figure 1.

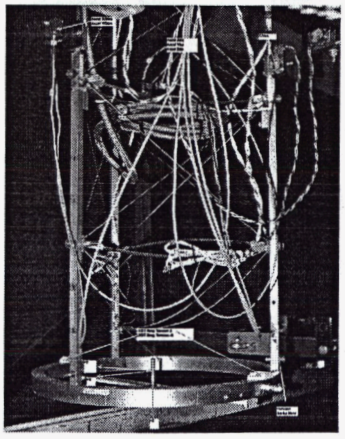

Figure 1. Tip Image With Tip Ring

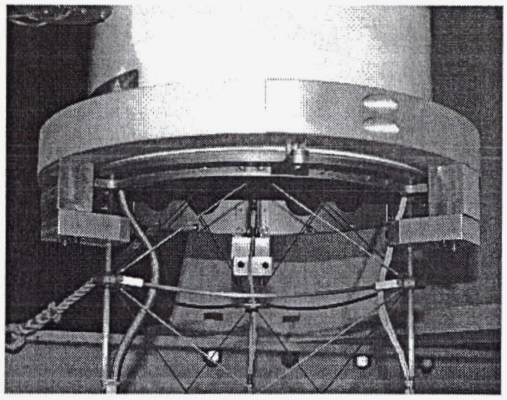

Figure 2. Longeron Clamps

In addition to the above modifications, the mast was further modified for this study by retrofitting a longeron clamp to impose a clamped condition at the canister/mast interface as shown in Figure 2.

OVERVIEW

Experiments were carried out to obtain static bending stiffness data, static torsional stiffness data, and bending/torsional modal data at mast lengths L=10 (M), L=22.5(M), and L=30(M), with constant loading cable tensions (see Figure 3) at T_c = 0 lb, 5 lb, and10 (lb). From

this test data, one can identify natural frequencies, mode shapes, and damping ratios that represent the dynamic behavior of the system. To minimize gravity effects, the boom was supported such that its longitudinal (z) axis is vertical at rest.

BOUNDARY CONDITIONS

As shown in Figure 2, clamps were installed between the motorized canister that holds the retractable boom and each longeron to force boundary conditions of the mast to be close to those of the booms of a typical solar-sail spacecraft. Accordingly, clamped-free boundary conditions, little-or-no tip mass and axial tension due to cables attached at approximately 45° to the longtitidinal axis at the interface between the stiffener section and the mast (see Figure 3) of a solar-sail mast were approximated.

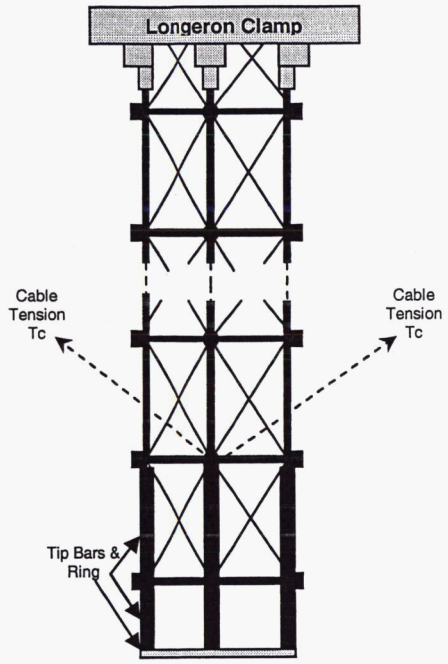

Figure 3. Axial Loading Configuration

ATTACHED INSTRUMENTS

Displacement

In all cases, displacement was measured at (4 or 8) measurement points distributed along the longeron to which the transverse bending forces were applied. Displacement sensors included Spring Return DC Position Sensors, also known as Linear Variable Differential Transformer (LVDT) Displacement Transducers and Ultrasonic Displacement sensors also known as UDI sensors. Displacement sensors were set up to measure beam displacement in the y-axis direction. For torsion tests, a pair of LVDT sensors measured angular rotation of the tip-ring.

Acceleration

Similarly, bi-axial accelerometers were used to measure x and y axis accelerations in response to y-axis forces or z-axis torques applied at the beam tip. Accordingly, these accelerometers were attached at roughly the same sensor locations as the displacement sensors. In addition, a tri-axial accelerometer, was installed on the longitudinal axis at the interface between the mast and stiffener section. This accelerometer is oriented to measure accelerations in the x, y and z axis direction at its location.

BENDING TESTS

Static Linear Displacement Tests

Static Stiffness data was obtained by recording y-axis displacement at multiple points on the mast as a constant transverse force, with multiple steps of varying magnitude, was applied to the beam tip in the y-axis direction. Direction of the force was reversed and the test was repeated. In each case input/output data was recorded. Output data was linear displacement in the y-axis direction at multiple points (including the tip) along the beam. This test was performed at 10(M), 22.5(M) and 30(M) deployment lengths without any externally induced axial loads. At the 22.5(M) deployment length, the test was repeated when axial loads were applied to the beam via two "loading cables" each of which had 5(lb) or 10(lb) tension T_c. Data from these tests were used to estimate bending stiffness *EI*.

Cut-Wire Tests

These tests are designed to capture dynamic response of the beam to an initial, linear, static displacement. This is achieved by attaching a wire to the beam tip, and pulling the wire in the y axis direction to induce a displacement at the beam tip. This displacement was preserved by maintaining a constant tension in the wire. Consequently, the beam has a fixed initial deflection. After the beam stabilized, the wire was suddenly cut causing the beam to vibrate. Time history of cable tension and beam response (displacement and acceleration) at sensor points was recorded.

Impact Tests

A tuned impact hammer was used to strike the beam in the y-axis direction at the stiffener section. Response (y-axis acceleration) of the beam at the measurement points were recorded and used for modal analysis. Several data sets were collected.

TORSION TESTS

Unlike bending tests, the tip ring was added to the free end of the stiffener section to facilitate application of torsional loads and measurement of angular response. As described earlier, the tip ring constrained the beam tip to pure z-axis rotation (see Figure 2).

Static Angular Displacement Tests

Static stiffness data was obtained by recording z-axis angular displacement at the tip-ring as a constant z-axis torque, with multiple steps of varying magnitude, was applied to the tip ring. Torque direction was reversed and the test was repeated. In each case input/output data was recorded. Output/response data was z-axis angular displacement at the beam tip. This test was performed at the 30(M) deployment length without any externally induced axial loads. Data from these tests was used to estimate torsional stiffness *GJ*.

Cut-Wire Tests

Similar to the bending test case, this is achieved by attaching a wire to the tip-ring, and pulling the wire to induce a z-axis torque at the beam tip. This displacement was maintained by keeping a constant tension in the wire. Consequently, the beam had a fixed initial angular deflection. Once the beam stabilized, the wire was suddenly cut which caused angular beam vibrations. Time history data of the cable tension and beam response (displacement and acceleration) at sensor points were recorded.

Impact Tests

A tuned impact hammer was used to strike the beam at the stiffener section in a direction that induces a z-axis torque. Response (z-axis angular acceleration) of the beam was measured and used for modal analysis. Since the Bi-axial accelerometers are offset from the *neutral* (z) axis, they measure radial and tangential acceleration along the beam. Consequently, they were used to estimate the z axis (angular) acceleration induced by the impact hammer.

BEAM PARAMETERS

In this section, we state parameters required to complete mathematical models provided in the next section. These parameters include mass-per-unit-length for the beam and tip-ring, buckling load, and maximum permissible tension in cables for applying axial load. For easy reference, these parameters are tabulated in Table 1.

Table 1. Summary of Parameters

Mast (beam excluding stiffener section & tip ring) Axial Length Bending Stiffness *EI* Torsional Stiffness *GJ*	 1181.5 (in) 19.87×10^6 (lb.in^2) 4.36×10^5 (lb.in^2)
Stiffener Section (between mast and tip ting): Axial Length	15.5 (in)
Tip Ring: Axial Length	7/8 (in)

BENDING STIFFNESS, EI, DETERMINATION

We assume the boom has a constant stiffness, *EI*, that is independent of beam length. Such a constant bending stiffness was provided by ABLE and is shown in Table 1. In this section, experimental verification of the constant bending stiffness is attempted. Verification of constant stiffness, *EI*, is done by analytically computing *EI* values at different deployed lengths from sets of static test data. Each test data set represents the transverse deflection profile of the boom for a specific transverse tip force. Transverse force was gradually increased and decreased in steps to collect the entire data set. There were a total of 18-42 good data sets depending on the configuration. Unlike mathematical models, the experimental data can be significantly influenced by gravity and it prevents a computation of the correct EI value of long (or heavy) structures. Thus, we developed a formula to accommodate this. Throughout this paper, we make the following standing assumptions.

Assumption 1:

1. Boom has a uniform mass stiffness, i.e. *m(s)=m* and *EI(s)=EI* respectively.
2. Perfectly straight beam.
3. External forces and moments do not induce any torsional effects.

The standard formula to compute EI under zero gravity assumption is:

$$EI_g^{(L)} = \frac{F(L) \cdot L^3}{3 \cdot y(L)} \tag{1}$$

It is expected that experimental data collected from static tests will be distorted by gravity. This gravity influenced test data will certainly affect EI values estimated using eq. (1). Thus, we developed a new formula that accounts for the case where axial and gravity loads exist. Assuming that the axial load considered here is due to a constant vertical force, *T(L)*, acting at the beam tip pointing in the positive s-direction and the beam profile may be approximated by a 3rd order polynomial

$$y(s) = c_0 + c_1 s + c_2 s^2 + c_3 s^3 \tag{2}$$

of the spatial coordinate $s \in [0, L]$, $c_k, k = 0,1,2,3$ are known coefficients and $y(s)$ represents the boom profile represented by experimental data, the standard stiffness formula is modified to[5],

$$EI^{(L)} = \frac{1}{2c_2}\left[F(L) \cdot L - T(L) \cdot y(L) - m \cdot g \sum_{k=1}^{3} \frac{c_k}{k+1} \right]. \tag{3}$$

At each length, 18-45 EI values were computed depending on numbers of available sets of data. The following table shows average values for each length.

COMPARISON OF EI VALUES

Table 2. Average Bending Stiffness Values (No-Axial Load Applied)

Boom Length (Meters)	$EI_g^{(L)}$ (Newton.Meter)	$EI^{(L)}$ (Newton.Meter)
L=10	4.5428×10^4	3.5262×10^4
L=22.5	7.9643×10^4	5.8976×10^4
L=30	1.2363×10^5	1.0239×10^5

Remark: Bending stiffness *EI* values computed at a fixed length are scattered in a range. Furthermore, *EI* values estimated at each length do not always lie in the same range of values. We are therefore unable to trust *EI* values estimated from static test data. Interestingly, the single *EI* value provided by ABLE, is close to the estimated *EI* values at 10(M) and 22.5(M) deployment lengths. Therefore, in the rest of the analysis, we assumed the boom has a constant and uniform *EI* value that is equal to the *EI* value of 5.7020×10^4 ($N.M^2$) provided by ABLE.

MATHEMATICAL MODELS

Assumption 2

1. Cross-sectional dimensions are small compared to beam length. Note that shear and rotary inertia effects can be neglected under this assumption[6]. However, these effects become significant as mode number increases[6].

2. Small bending deformations, specifically: $\left(\frac{dy}{ds}\right)^2 << 1$.

3. The beam is stiff in the axial direction, so length change due to axial forces is negligible.

EQUATION OF MOTION: BENDING

We considered a beam clamped at one end and free at the other end and derived equations of transverse motion $y(s,t)$ in response to applied forces and moments. At rest, the beam is vertical to minimize gravity effects and thereby simulate the zero gravity effects of space. Note that we assumed the beam is uniform and lacks a tip-mass in bending motion. The beam under investigation assumes there is no axial motion and its equation of motion is[5],

$$\frac{\partial^2}{\partial s^2}\left[EI\frac{\partial^2 y}{\partial s^2}\right] - T(L)\frac{\partial^2 y}{\partial s^2} + mg\left((s-L)\frac{\partial^2 y}{\partial s^2} + \frac{\partial y}{\partial s}\right) + m\frac{\partial^2 y}{\partial t^2} = w(s,t). \qquad (4)$$

Note that if *T(L)=w(s,t)=0,* the expression above corresponds to "case 2" of the Rakoczy model[9].

We used *admissible* functions in our analysis because of difficulties computing the analytical mode shape functions $\phi_j(s)$. The *admissible* functions are the mode shape functions of the classical Euler-Bernoulli Beam, i.e:

$$u_j(s) = c_{1j}\sin(\beta_j s) + c_{2j}\cos(\beta_j s) + c_{3j}\sinh(\beta_j s) + c_{4j}\cosh(\beta_j s) \qquad (5)$$

where β_j, and c_{1j}, c_{2j}, c_{3j}, c_{4j}, $j = 1,2,3,...$ are computed from boundary conditions.

TORSION MODEL WITH TIP MASS

Assumption 2: Torsional stiffness of the beam is uniform (i.e *GJ(s)=GJ* with known *GJ*).

A mathematical model depicting the beam in torsion is standard and is provided below. Let $M_T(s,t)$ denote a distributed external torque, $\theta(s,t)$ angular rotation, G shear modulus, $J(s)$ a geometric property, GJ torsional stiffness and $I(s)$ mass polar moment of inertia per unit length of the beam. The differential equation of motion is[6]

$$I(s)\frac{\partial^2\theta(s,t)}{\partial t^2}-\frac{\partial}{\partial s}\left[GJ\frac{\partial\theta(s,t)}{\partial s}\right]=M_T(s,t) \tag{6}$$

while the jth mode shape function ϕ_j is,

$$\phi_j = c_j \sin(\beta_j s). \tag{7}$$

DATA ANALYSIS

The data analysis consists of using the mathematical model to predict (1) natural frequencies and (2) mode shapes of the first three modes. The analysis is completed by comparing these predicted natural frequencies and mode shapes with those measured from experimental data for a corresponding configuration (deployment length and axial load). This analysis is repeated for every test configuration.

DATA ANALYSIS: BENDING MOTION

From the impulse response due to the transverse forces induced by the impact hammer, the modal parameters, the corresponding natural frequencies predicted by the mathematical model (Table 3), and the damping ratios from the impact tests (Table 4) are tabulated below.

Table 3. Experimentally Obtained/Model Predicted Natural Frequencies

		Experimentally Obtained			Model Predicted		
L (Meters)	T_c (lb)	f_1 (Hz)	f_2 (Hz)	f_3 (Hz)	F_1 (Hz)	f_2 (Hz)	f_3 (Hz)
10	0	1.0990	6.3965	N/A	1.3454	8.2999	22.9846
22.5	0	0.2819	1.5602	3.7780	0.3155	1.6825	4.7204
22.5	5	0.5574	1.6124	N/A	0.3047	1.6671	4.7074
22.5	10	0.7030	1.6175	N/Av	0.2932	1.6515	4.6944
30	0	0.2180	0.9260	2.4300	0.2123	0.9582	2.7014
30	5	0.3452	0.9549	2.4952	0.2043	0.9424	2.6883
30	10	0.4187	0.9846	2.4547	0.1959	0.9263	2.6752

Table 4. Damping Ratios Obtained from Experimental Data for Bending Motion

L (Meters)	T_c (lb)	ζ_1 (Hz)	ζ_2 (Hz)	ζ_3 (Hz)
10	0	0.0125	0.0343	N/A
22.5	0	0.0141	0.0142	0.0388
22.5	5	0. 0114	0.0119	N/A
22.5	10	0. 0068	0.0190	N/A
30	0	0. 0420	0. 0160	0.0250
30	5	0. 0081	0. 0110	0.0160
30	10	0. 0126	0. 0133	0.0226

Figures 4-10 compares model predicted mode shape and mode shape reconstructed from experimental data. Our analysis is limited to the first three modes because they account for most of the beams vibration motion. Note that sometimes, no reliable data was available to construct the mode shape of the third mode. These figures show that the predictions are reasonably accurate.

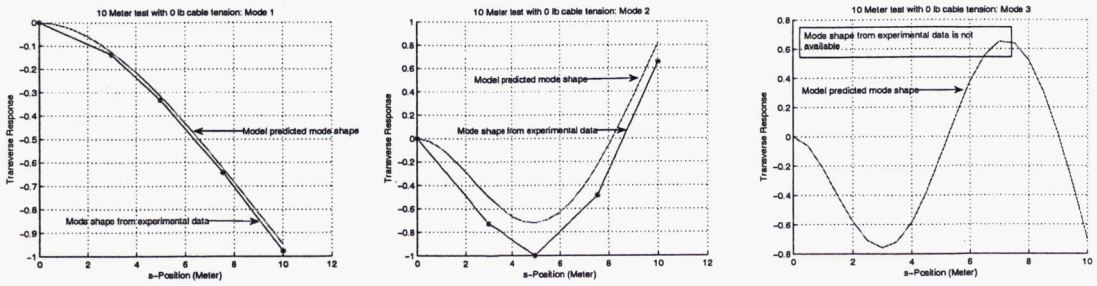

Figure 4. 10 Meter Test with 0 lb cable tension

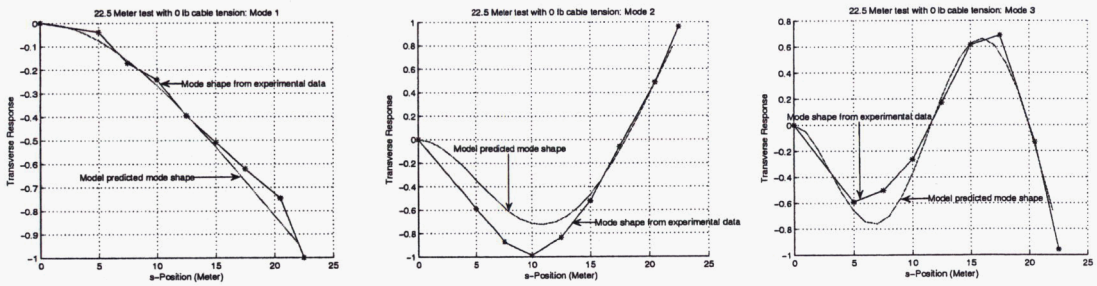

Figure 5. 22.5 Meter Test with 0 lb cable tension

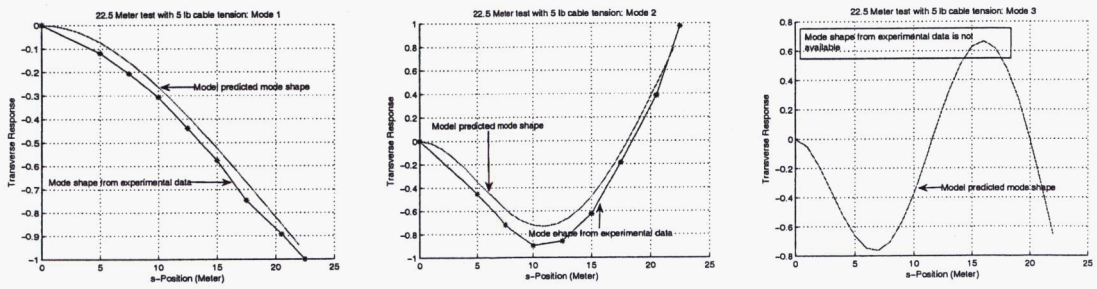

Figure 6. 22.5 Meter Test with 5 lb cable tension

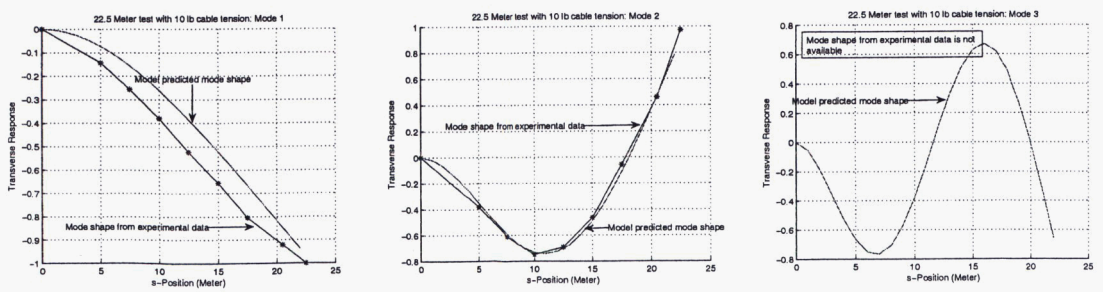

Figure 7. 22.5 Meter Test with 10 lb cable tension

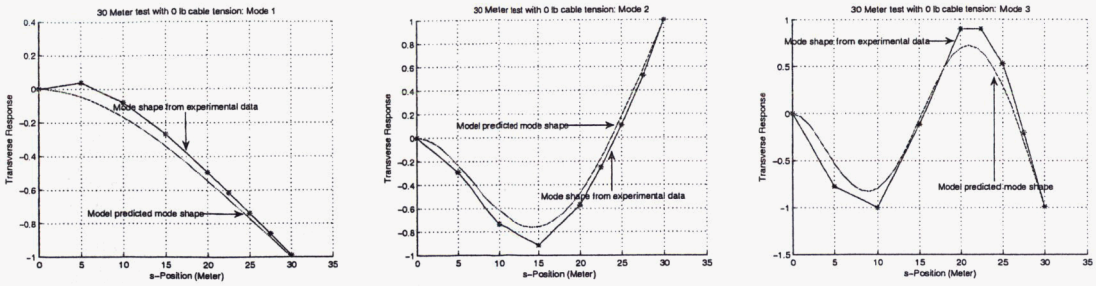

Figure 8. 30 Meter Test with 0 lb cable tension

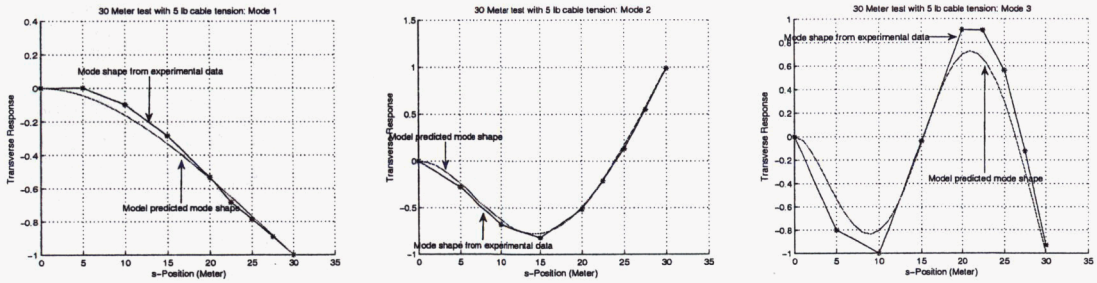

Figure 9. 30 Meter Test with 5 lb cable tension

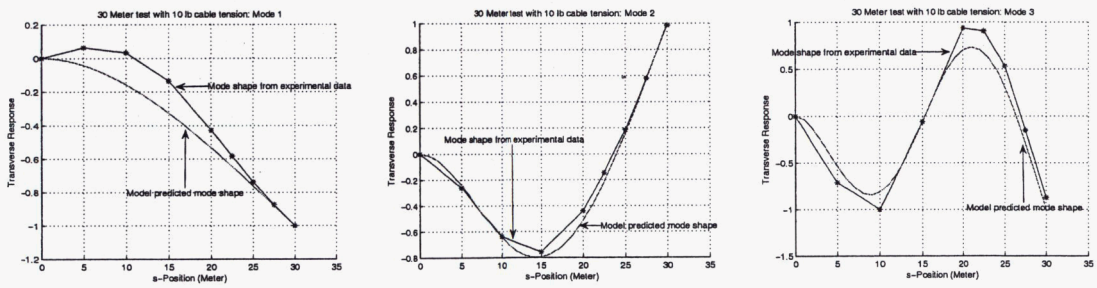

Figure 10. 30 Meter Test with 10 lb cable tension

We pay particular attention to Figures 11 and 12 which depict the changes of mode shapes with regard to different tension load being applied. As expected, the mode shapes of the mathematical models show resilient behavior with respect to the changes of tension load. However, notable changes are shown in mode shapes constructed from the experimental data. Further discussion will be given in the next section.

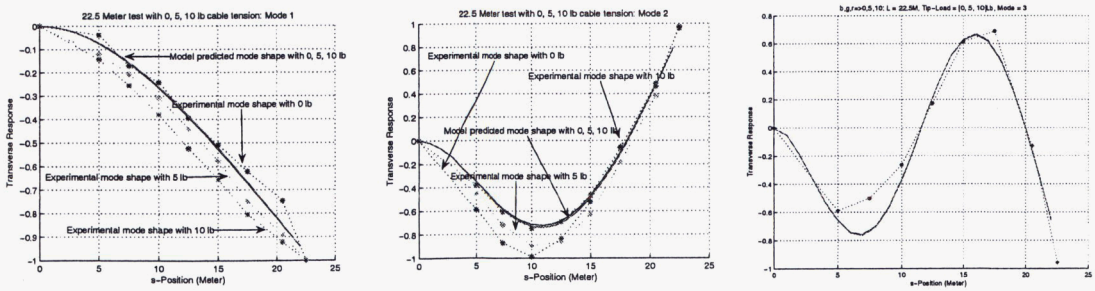

Figure 11. 22.5 Meter Test with 0, 5, 10 lb cable tension

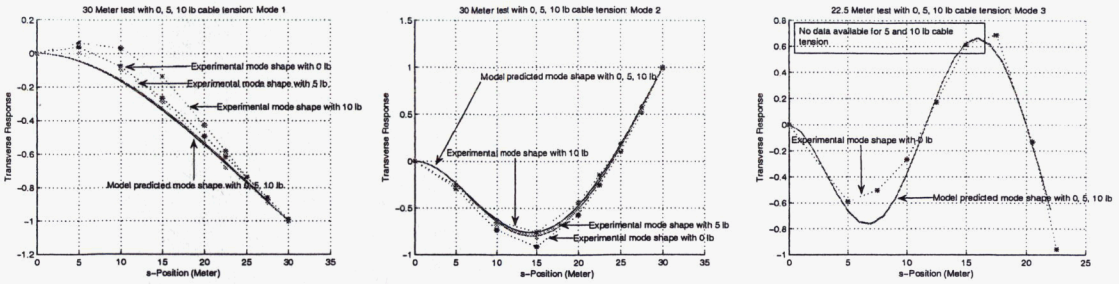

Figure 12. 30 Meter Test with 0, 5, 10 lb cable tension

DATA ANALYSIS: TORSIONAL MOTION

The Natural frequencies predicted by the mathematical model are provided below.

Table 6. Model Predicted Natural Frequencies for Torsional Motion

Length L (Meters)	Cable Tension T_c (lb)	f_1 (Hz)	f_2 (Hz)	f_3 (Hz)
30	0	1.6934	5.0803	8.4672

Unfortunately, the corresponding experimental torsional natural frequencies and mode shapes are not available due to the inability to obtain reliable torsional data. This issue will be discussed further in the next section. Consequently, the natural frequencies of the mathematical model in Table 6, and the corresponding mode shapes (not shown) cannot be validated.

Despite the failure to obtain mode shape functions from the torsion data collected, FRF data obtained from z-axis torque (input) at the free (for rotation) end plus z-axis acceleration (output at the free end) was adequate for some crude analysis. FRF data from the modal analysis was compared with FRF data from the mathematical model. These two FRFs are depicted in Figure 12. A crude estimate of the first three natural frequencies was made as follows. The frequencies at which the first three magnitude peaks (accompanied by 180° (deg) Phase shifts) occur was determined visually. These crude natural frequency estimates are provided in Table 7.

Table 7. Rough Estimates of Experimental Natural Frequencies for Angular Vibration

Length L (Meters)	Cable Tension T_c (lb)	f_1 (Hz)	f_2 (Hz)	f_3 (Hz)
30	0	1.91	5.64	9.38

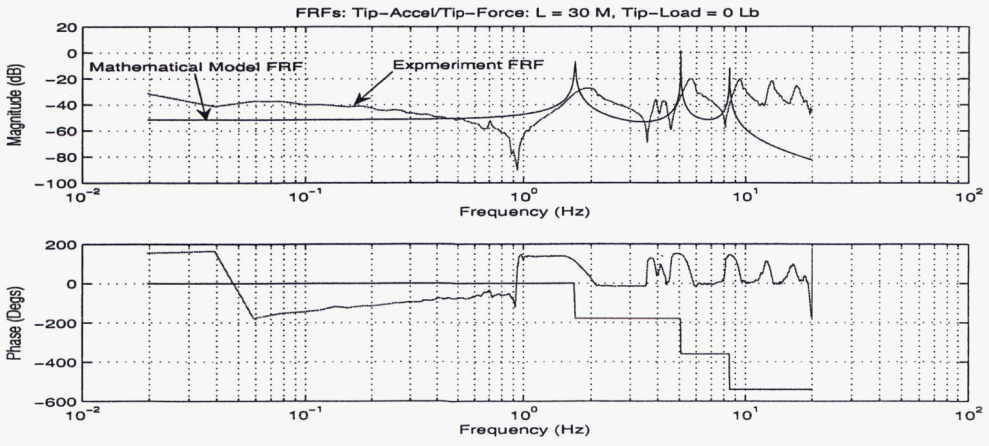

Figure 13. Torsion: Experimental and Mathematical Model FRFs

DISCUSSION

In this section, we discuss some of the issues raised during the data analysis including reliability of the data due to limitations of the experimental setup.

EXPERIMENTAL SETUP

1. The 30 meter boom under study is not perfectly straight and has a slight "bow". This causes an inevitable coupling between bending and torsion motions. Consequently, the "bow" in our boom guarantees that Torsion and Bending modes will always be *coupled*.[6] However, the study assumes the boom is perfectly straight and bending and torsion motions are completely decoupled. The mathematical models we developed are based on this assumption.
2. As described earlier, the boom has a stiffener section (see Figure 2) at the end. Since we assume the boom is long and slender, we expect the effect of the stiffener section becomes insignificant as the length of the boom increases.

BENDING STIFFNESS VALUE

Based on the literature provided by ABLE (manufacturer of the boom under consideration), we assumed the boom has a uniform stiffness. In fact, the entire analysis performed here is based on a mathematical model with the constant stiffness value provided by ABLE. Initially, attempts were made to verify this central assumption from static test data sets obtained from experiments. As discussed in the *bending stiffness determination* section, a conclusive verification was not achieved. Some of the observations made from our analysis of the experimental data are:

1. The standard formula in eq. (1) was problematic when it utilized static test data that was significantly influenced by gravity. Consequently, the *EI* values computed with this formula increased as the length increases as shown in Table 2. Since the formula in eq. (1) assumes zero gravity condition and the gravity effects on the data is increasing as the length of the boom increases, the constant/accurate *EI* cannot be obtained if such gravity influences on the apparent stiffness is large.
2. A new formula was derived to mathematically remove gravity influences from the static test data. As shown in Table 2, the results show that the constant/accurate *EI* was still not attainable from the static test data even after removing gravity effects. Therefore, we failed to experimentally verify the primary assumption we made based on ABLE's literature.

MODE SHAPE FUNCTIONS

Comparing mode shape functions predicted by the mathematical model against mode shapes reconstructed from experimental data, we observed the following.

1. Mathematically predicted mode shape functions generally agree with experimental shapes.
2. Modal analysis of experimental data often failed to identify higher modes. As a result, some test configurations lack a third mode for data analysis.
3. The modal analysis also had difficulty identifying any torsional modes from experimental data.. As a result, data analysis for torsional motion was done only with the mathematical model and was therefore limited.
4. It is well known that natural frequency should decrease with an increase in compressive load. This trend was observed in our mathematical model as shown in Table 4. However, the experimental data generally showed the opposite trend. Such an unreasonable phenomena may indicate inaccuracy of the test data.
5. The difference between natural frequencies predicted by the mathematical model and natural frequencies measured from experimental data generally reduced as the boom length increased. This is an expected outcome because the beam should become a slender beam (as assumed in the mathematical model) as it's length increases. Also, the effects of the unmodeled stiffener section should become less significant as length increases.

EFFECTS OF AXIAL LOADS ON MODE SHAPE FUNCTIONS

Mode shapes of a clamped free beam are a function of axial load, but the change in mode shape produced by a large change in axial load is generally very small[2]. Consequently, we expected the mode shapes predicted by our mathematical model and mode shapes estimated from experimental data would both show insignificant changes to small (compared to buckling load) axial load changes. As expected, mode shapes predicted by the mathematical models hardly changed with axial load. However, experimental mode shapes changed significantly for relatively small axial loads. Unfortunately, a thorough investigation of the cause(s) of this discrepancy will require additional experiments and mathematical analysis that are beyond the scope of our study. In the absence of this, two likely sources of this anomaly are suggested below.

The beam contains a significant bow (global deformation) that is visible to the naked eye when the boom is in an unloaded state. Consequently, the bending and torsional vibration modes will always be coupled[6]. Therefore, the vibration modes determined from transverse vibration data are actually a combination of bending modes coupled with angular motion. As a result, the apparent change in the experimental transverse mode shapes with axial tension may be due to coupling effects. On the other hand, the mathematical model assumes a perfectly straight beam and is therefore free of coupling effects.

At short lengths a coilable boom is generally a very predictable and readilly modelled linear structure[7]. However, ultra light weight booms with long lengths are particularly susceptible to stiffness and therefore strength reduction due to local longeron and global mast waviness[3,7,8].

However, our mathematical mode shape functions were derived assuming the beam is perfectly straight, and its bending stiffness is uniform and constant. Therefore, the existence of a significant bow invalidates this assumption. In fact, our inability to determine a constant and uniform stiffness *EI* value from static test data *may* actually be due to the effects of local/global stiffness changes caused by an imperfectly straight boom.

NATURAL FREQUENCIES

1. As stated earlier, the boom was assumed to be uniform for the bending model. However, we know the boom was much stiffer and much heavier at the last two bays. From simple math models of the first frequency of a beam with a tip mass, we know that the mass of the tip mass has a much more significant effect on the first mode frequency than the mass of the entire boom[2]. This may explain the large discrepancy between the experimental and math model first mode frequency.
2. Pure Torsion Mode shapes and frequencies could not be determined from experimental data because of the coupling between the Torsion and Bending Modes.

CONCLUDING REMARKS

The question we asked in this study was: can the dynamic behavior of an extremely large solar-sail spacecraft be predicted by a standard scalable mathematical model? We attempted to answer the question by validating the mathematical model against data collected from experiments conducted on a 30 (Meter) boom in various lengths. As we discussed above, the results are not definitive and conclusive. However, evidence generally suggests that simple linear-time invariant mathematical models can predict dynamic behavior of a long boom that is similar to the one used in this study. It seems that most of the mismatches are due to inability of the experimental environment to satisfy some of the assumptions made in developing theoretical models. Although some of these assumptions are expected to be satisfied more closely in real flight conditions (zero gravity, much longer booms, etc.), one of the most critical questions to be asked may be whether a boom satisfies the perfectly straight beam assumption.

Depending on degree of waviness, one may have to drop this assumption and develop complicated models that represent coupling between bending and torsional motion. In any case,

some form of robust control to overcome the difference between analytical models and the physical structures will be necessary.

ACKNOWLEDGMENT

The work described in this paper was funded in whole or in part by the In-Space Propulsion Technology Program, which is managed by NASA's Science Mission Directorate in Washington, D.C., and implemented by the In-Space Propulsion Technology Project Office at Marshall Space Flight Center in Huntsville, Alabama. The program objective is to develop in-space propulsion technologies that can enable or benefit near and mid-term NASA space science missions by significantly reducing cost, mass or travel times.

REFERENCES

1. ***Automatically Deployable ABLE Booms***, AEC-ABLE Engineering Company, Inc, Goleta, CA.
2. R. D. Blevins, ***Formulas for Natural Frequency and Mode Shape***, pp. 146, 158, Van Nostrand Reinhold Company, New York, NY, 1979.
3. R. Crawford, J. Hedgepeth, "Effects of Initial Waviness on the Strength and Design of Built-up Structures", ***AIAA Journal***, pp. 672 - 675, Vol. 13, No. 5, 1975.
4. R. F. Crawford, and R. M. Warden, ***Final Acceptance Data Package for SAFE Mast Modification for CASES Program***, AECR90472/461, pg. 2, AEC-Able Engineering Company Inc., Goleta, CA., Feb., 1990.
5. L. H. Keel, and O. Adetona, "Model Correlation Study of a Retractable Boom for a Solar-sail Spacecraft ",Technical report submitted to Dr. Mark S. Whorton (NASA Technical Officer), EV42 / Guidance, Navigation, and Mission Analysis, NASA Marshall Space Flight Center, AL, September 14, 2005.
6. L. Meirovitch, ***Analytical Methods in Vibrations***, pp 135, 157, 166, 454, Macmillan Publishing Co, Inc, New York, NY, 1967.
7. D. M. Murphy, B. D. Macy, and J. L. Gasper, "Demonstration of a 10-M sail System", ***Proceedings of 45th AIAA/ASME/ASCE/AHS/ASC Structures, Structural Dynamics & Materials Conference***, pg. 4, Palm Springs, CA., 19-22 April, 2004.
8. D. Murphy, T. Trautt, M. McEachen, D. Messner, G. Laue, and P. Gierow, ``Progress and Plans for System Demonstration of a Scalable Square Solar Sail", ***Proc. 14th AAS/AIAA Space Flight Mechanics Conference***, pp 11-12, Maui, HI, February 8-12, 2004.
9. J. Rakoczy, "Experimental Verification of the equations of motion for a deployable flexible beam in one-g, Part 1: General equations of motion", ***ED12-92-141 Memorandum for record***, NASA Marshal Space Flight Center, AL.
10. ***http://www.aec-able.com/Booms/coilboom.html***

Model Correlation Study of A Retractable Boom for a Solar Sail Spacecraft

O. Adetona, L.H. Keel
Tennessee State University, Nashville, TN
J.O. Oakley, K. Kappus, M.S. Whorton, Y.K. Kim, J.M. Rakoczy
NASA-Marshall Space Flight Center, Huntsville, AL

Presented at 53th JANNAF, December 5-9, 2005
Hyatt Regency Monterey and Naval Postgraduate School, Monterey, CA.

Controls, Astrophysics and Structures Experiment in Space (CASES) Ground Test Facility

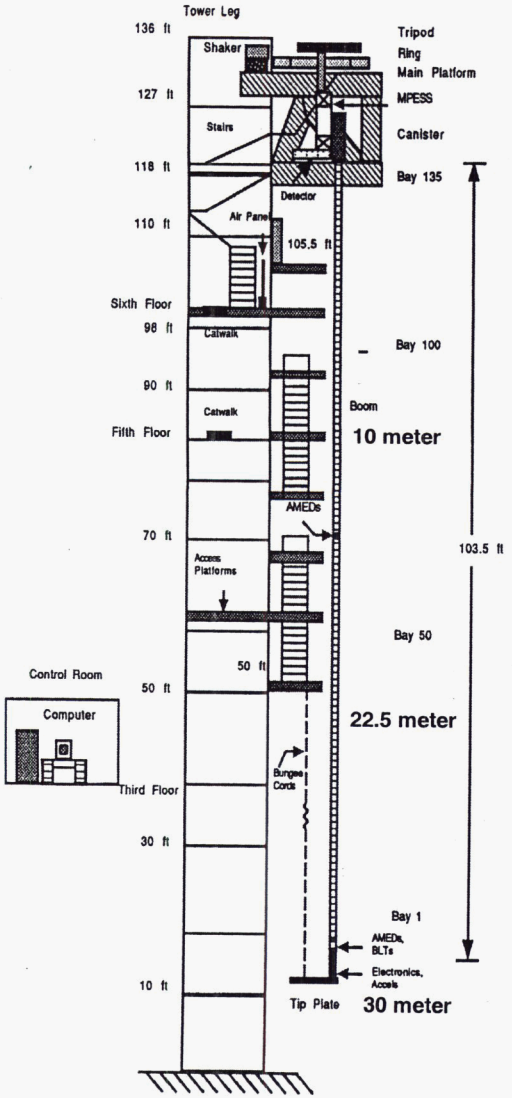

•Design, Fabrication & Modification of CASES Facility Structure to Provide a Rigid Support for the SAFE Mast Canister System

•Design & Fabrication of Longeron Clamping Bracket to Facilitate a Fixed-Base Cantilever Configuration of the Boom at Any Deployed Length.

I-Beam

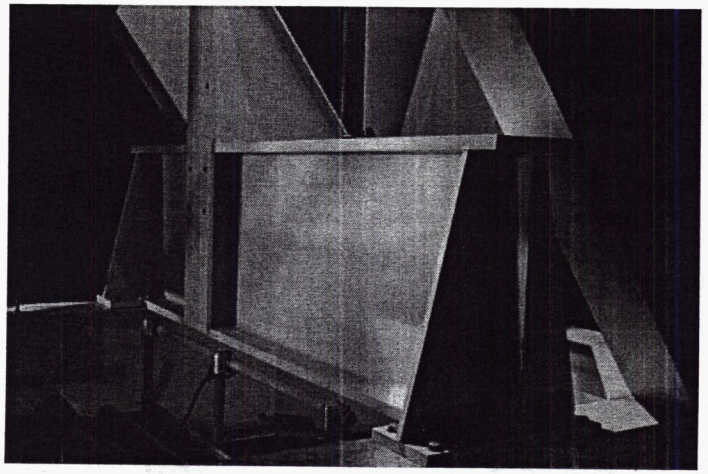

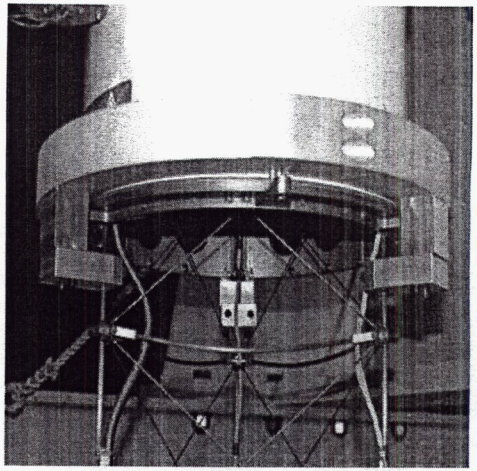

Longeron Clamping Bracket

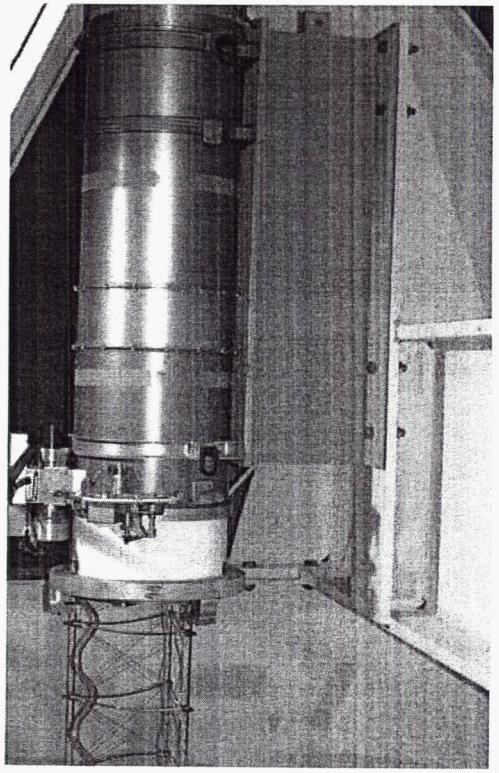

Mounted SAFE Mast Canister System

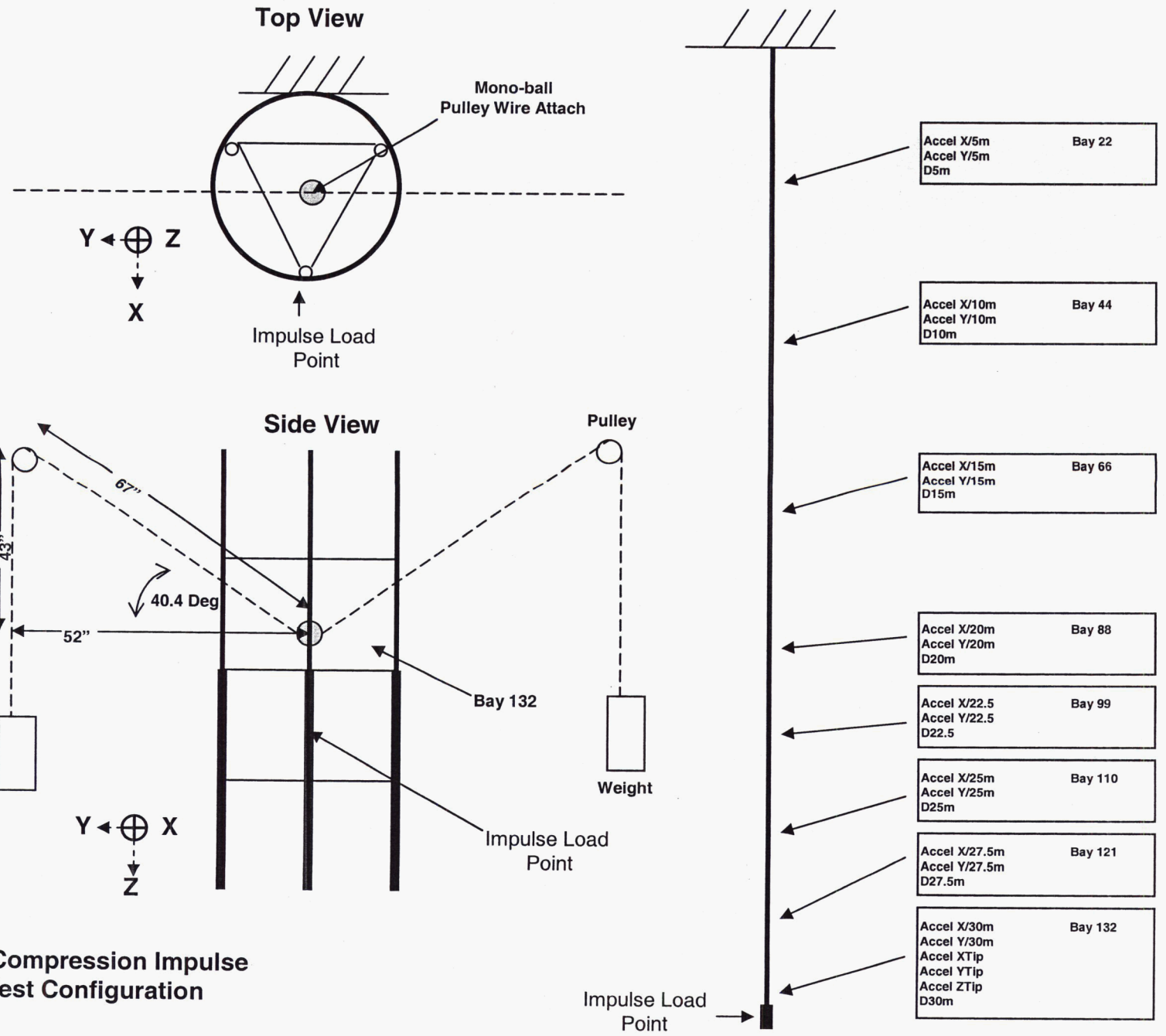

30m Compression Impulse Test Configuration

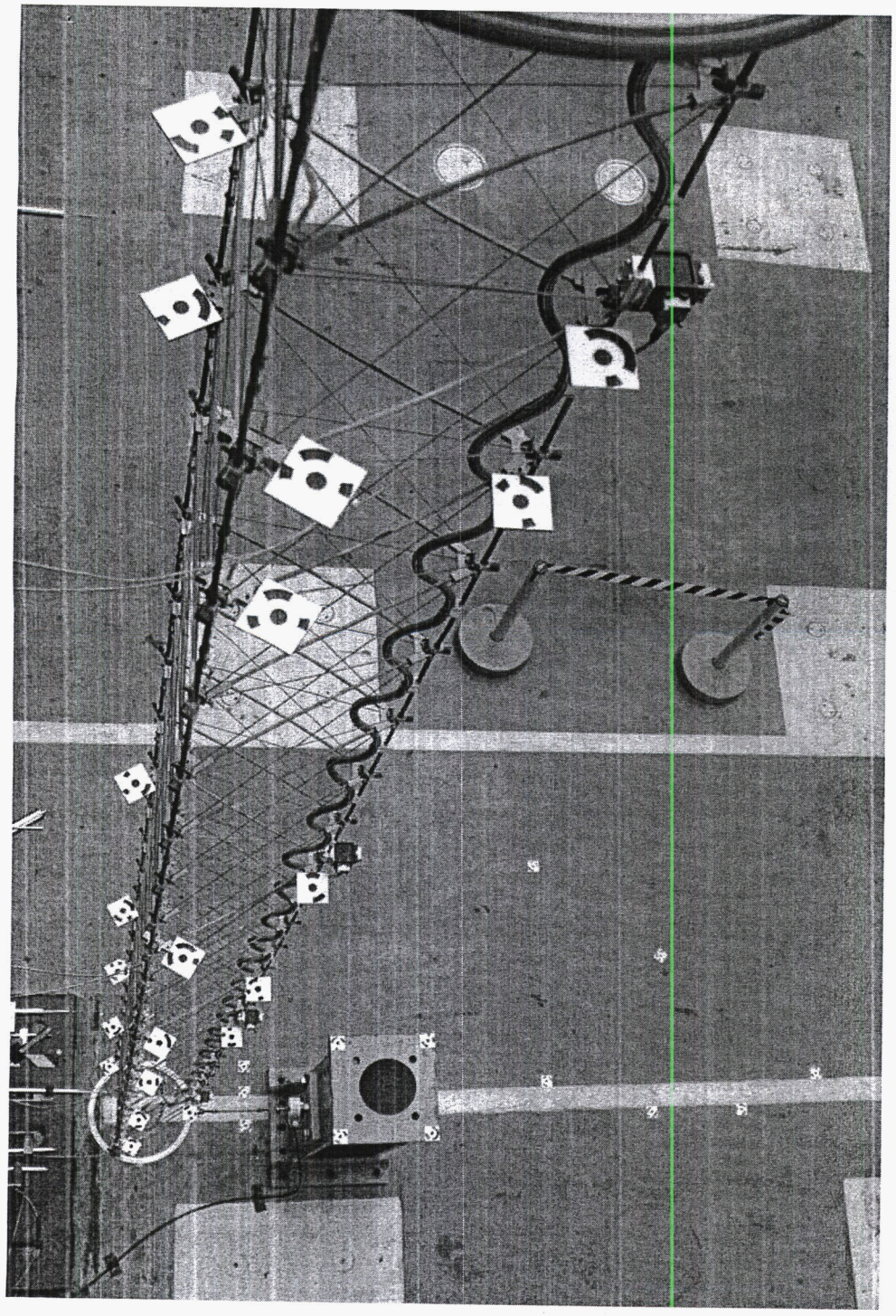

Boom Deployed at 5.5 m

Static Load/Deflection

Incremental loads were applied at the mast tip in the +X & -X directions by a load cell, turn-buckle & mono-ball system.
Flagged data scans of the applied load at the tip and deflection data at defined locations on the mast were acquired.

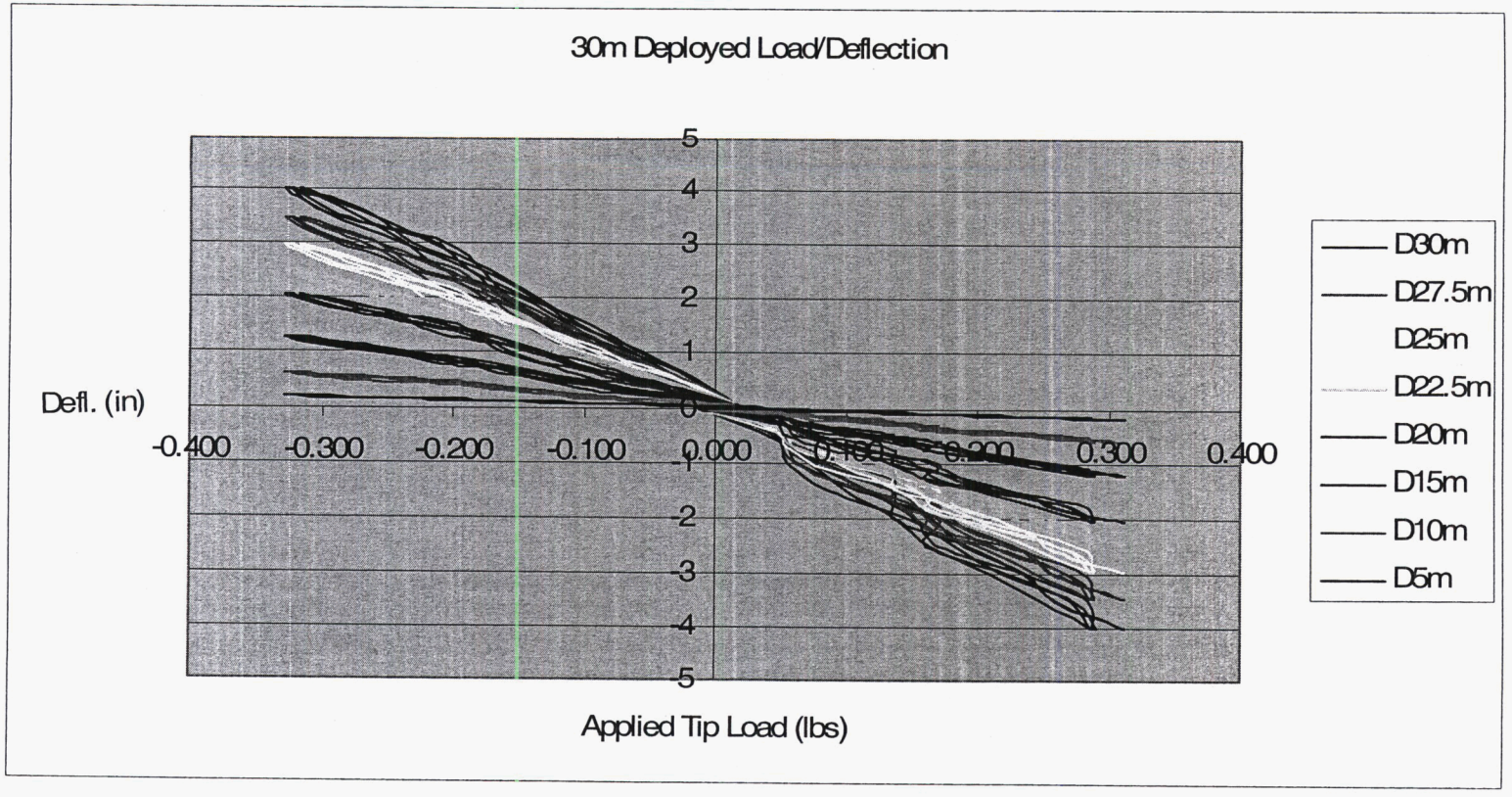

Scalability Study of the Boom

1. Develop mathematical models representing bending and torsion vibration, respectively.
2. Conduct experiments for 10M, 22.5M, and 30M booms under various axial loads.
3. Compare mode shape functions
4. Compare natural frequencies
5. Discussion & Remarks

Experimental Setup: Boom and Canister

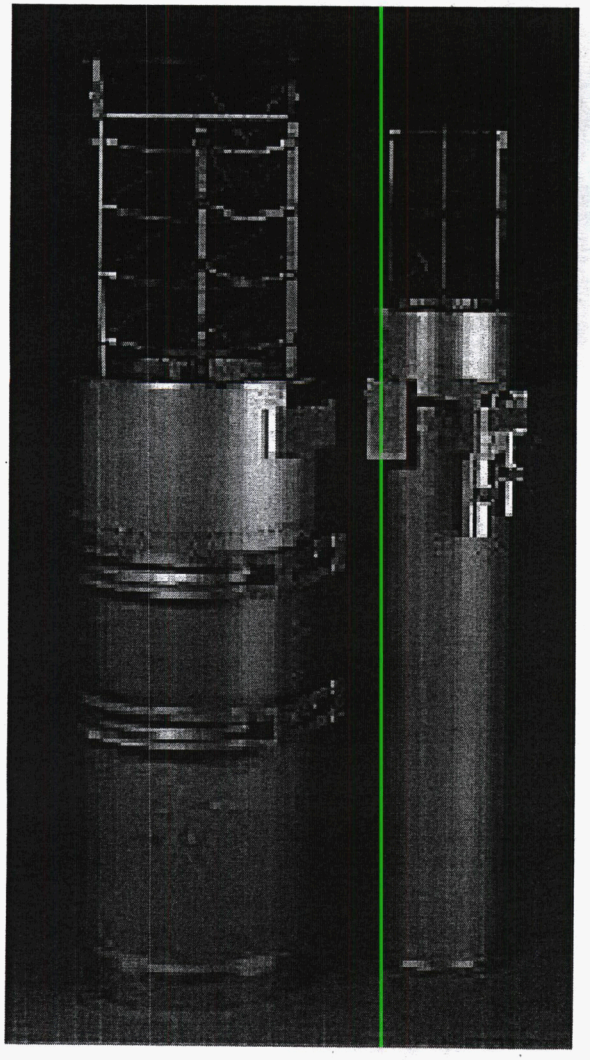

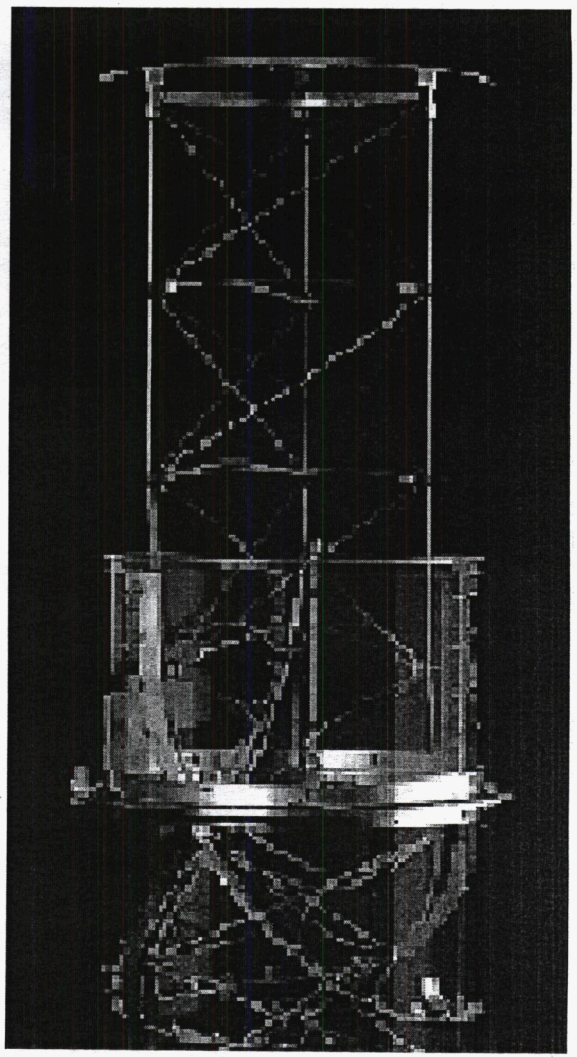

Tip of the boom for bending test

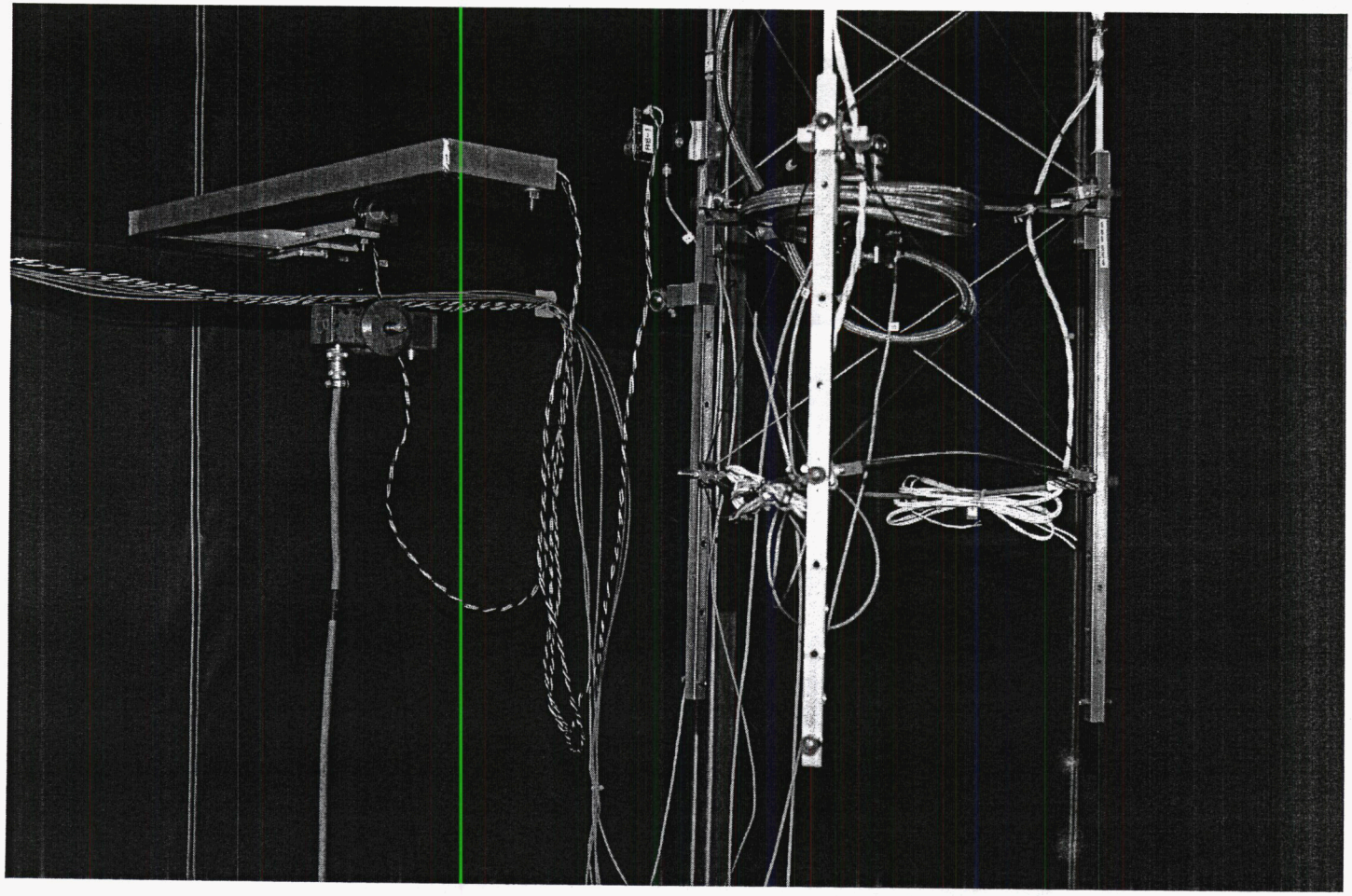

Tip of the boom for torsion test

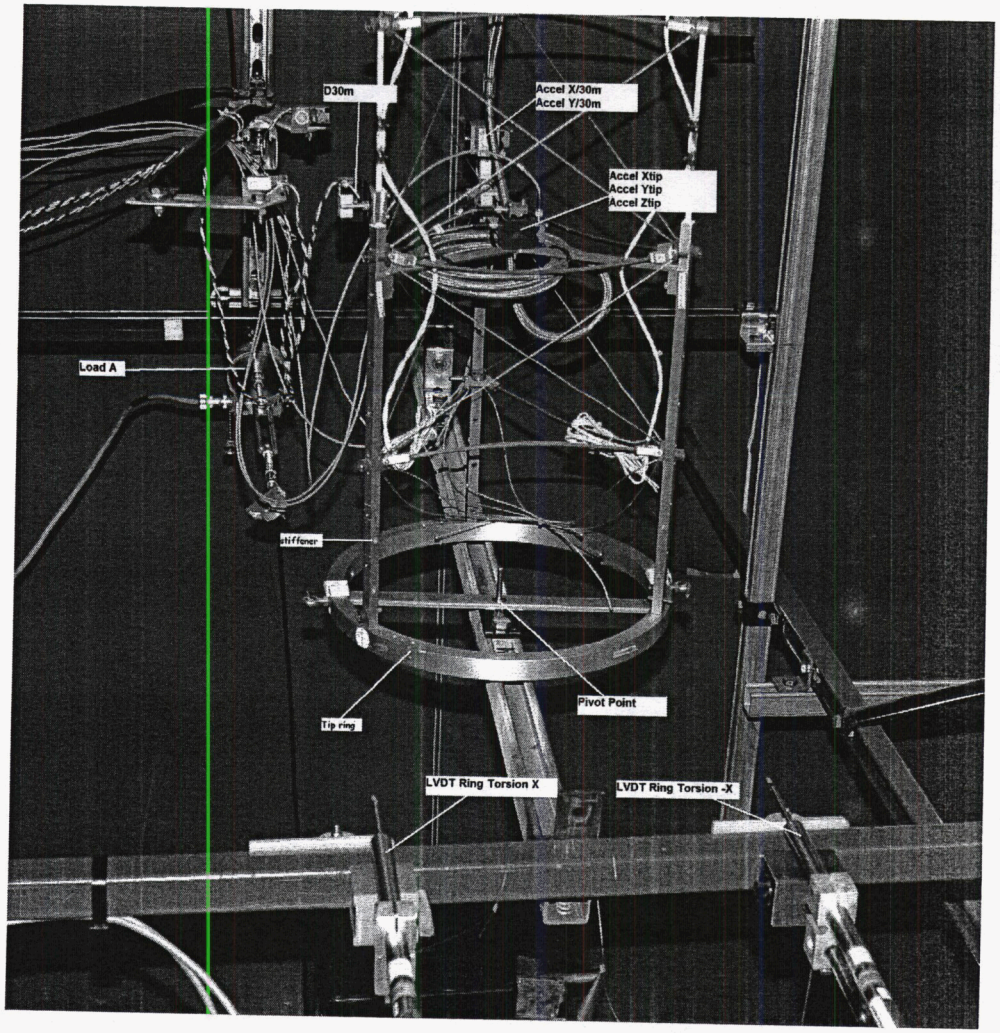

Experimental Setup: Overview

Experiments were carried out to obtain

- static stiffness data,
- static torsional stiffness data,
- bending/torsional modal data

at mast lengths of

- 10M, 22.5M, 30M

with constant loading cable tensions at

- 0 lb, 5 lb, 10 lb

Exp. Setup: Boundary Conditions

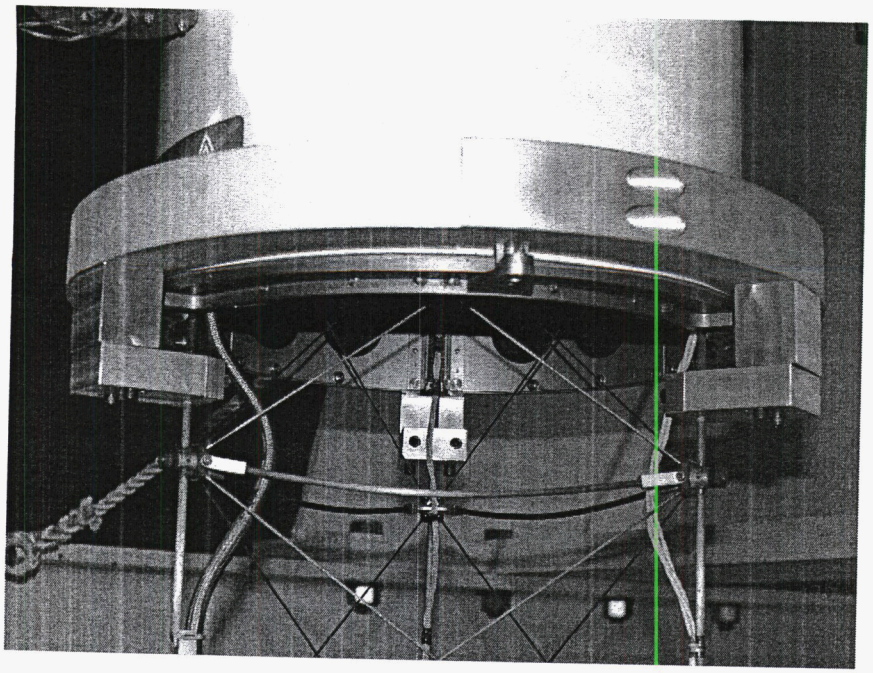

- Clamps were installed between the motorized canister of the boom and each longeron.
- It is to force boundary conditions of the mast to be close to those of the booms of a typical solar-sail spacecraft.

Exp. Setup: Axial Loading Configuration

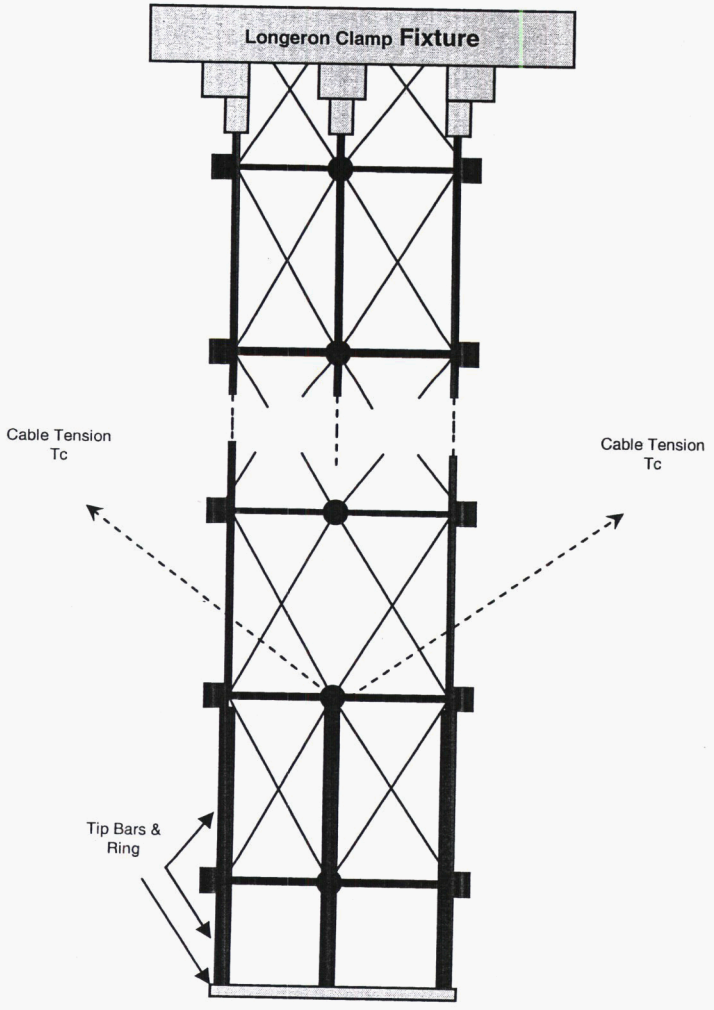

- Axial tension due to cables attached at approximately 45 degree to the longitudinal axis.
- Note that the stiffener section at the end of mast for end-attachment.

Exp. Setup: Attached Instruments

- Displacement: displacement was measured at 4 or 8 measurement points (depending on the length of boom) distributed along the longeron to which the transverse bending forces were applied.
- Displacement sensors: LVDT displacement transducers, UDI sensors
- Acceleration: bi-axial accelerometers were used to measure x and y axis accelerations in response to y-axis forces or z-axis torques applied at the beam tip.

Experimental Tasks

- Bending Tests
  - Static Linear Displacement Tests
  - Cut-Wire Tests
  - Impact Tests
- Torsion Tests
  - Static Angular Displacement Tests
  - Cut-Wire Tests
  - Impact Tests

EI determination

- Analytical Determination
  - Assumption:
    - Boom has a uniform mass stiffness
    - Perfectly straight beam
    - External forces and moments do not induce any torsional effects
  - Compute values by using static test data and the formula derived (see the paper)
  - Note that the gravity effects have been considered in the formula

- Compare with EI values provided by the ABLE (5.7020×10^4) Boom has a uniform mass stiffness

Average Bending Stiffness Values (No-Axial Load Applied)

Boom Length (Meters)	$EI_g^{(L)}$ (Newton.Meter)
L=10	4.5428×10^4
L=22.5	7.9643×10^4
L=30	1.2363×10^5

- At each length, 18-45 EI values were computed depending on number of available sets of data.
- As seen, estimated EI values are not constant.
- We are unable to trust any of these computed values.
- Therefore, in the rest of the analysis, we assumed the boom has a constant and uniform EI value that is equal to the value provided by the ABLE.

Mathematical Model

Mathematical models for bending and torsion are developed based on the following assumption

Assumption

- Cross-sectional dimensions are small compared to beam length (i.e., a long slender beam)
- The beam is stiff in the axial direction, so length change due to axial forces is negligible.
- Small bending deformation, specifically,

$$\left(\frac{dy(s)}{ds}\right)^2 << 1$$

Natural Frequency Comparison

Experimentally/Model Obtained Natural Frequencies for Bending Motion

Length L	Cable Tension	f_1 (Hz)	f_2 (Hz)	f_3 (Hz)
10	0	1.0990	6.3965	N/A
22.5	0	0.2819	1.5602	3.7780
22.5	5	0.5574	1.6124	N/A
22.5	10	0.7030	1.6175	N/A
30	0	0.2180	0.9260	2.4300
30	5	0.3452	0.9549	2.4952
30	10	0.4187	0.9846	2.4547
10	0	1.3454	8.2999	22.984
22.5	0	0.3155	1.6825	4.7204
22.5	5	0.3047	1.6671	4.7074
22.5	10	0.2932	1.6515	4.6944
30	0	0.2123	0.9582	2.7014
30	5	0.2043	0.9424	2.6883
30	10	0.1959	0.9263	2.6752

Data Analysis: Natural Frequencies

Transverse Vibration:

- In theory, natural frequencies should decrease as compression load increases.
  - Mathematical model shows such trend.
  - However, experiments generally shows opposite trend.
  - This led to a doubt of reliability of experimental data.
  - Due to inability to induce pure transverse motion.

- Natural Frequency difference between experiment and model reduced as length of the boom increases. This led us to believe the long slender beam assumption is better satisfied at longer lengths.

Angular Vibration:

* No experimental data available for angular vibration.

Data Analysis:
10 Meter test with 0 lb cable tension Mode Shape

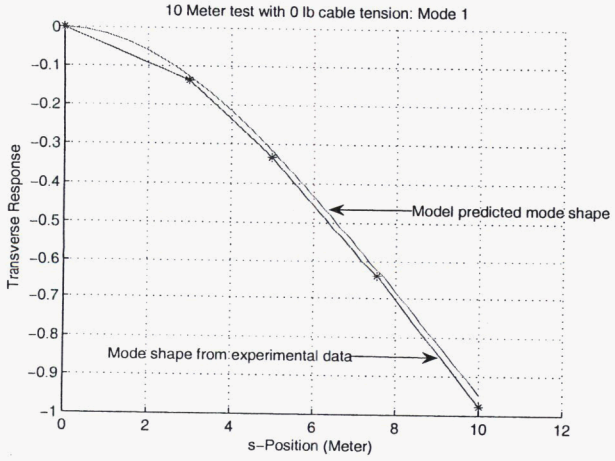

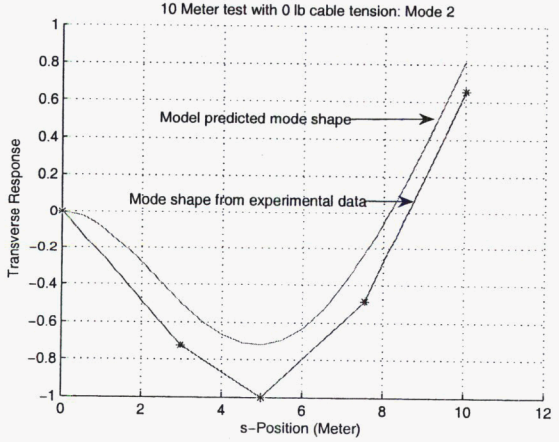

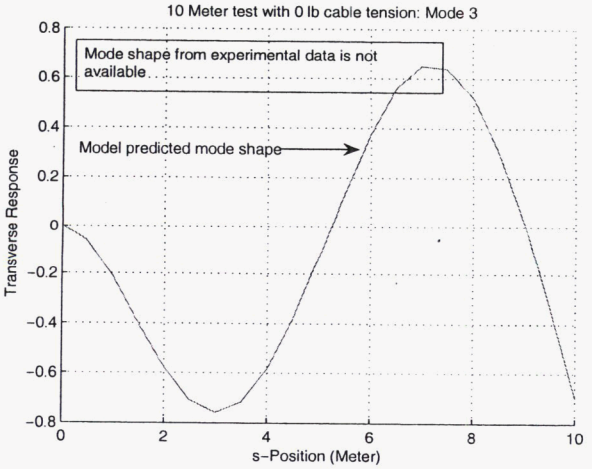

Data Analysis:
22.5 Meter test with 0 lb cable tension Mode Shape

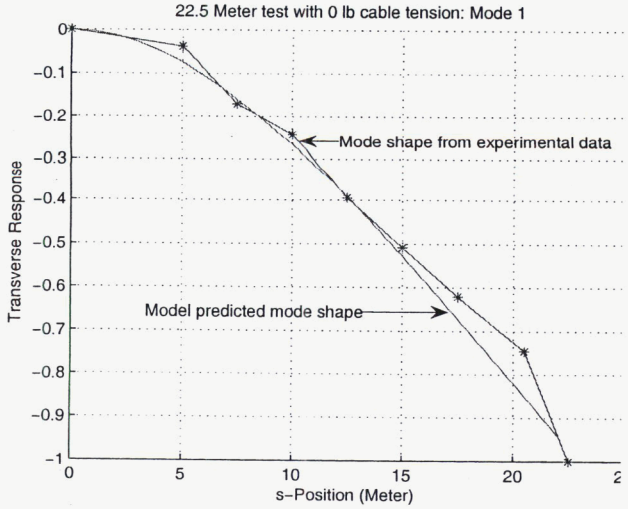

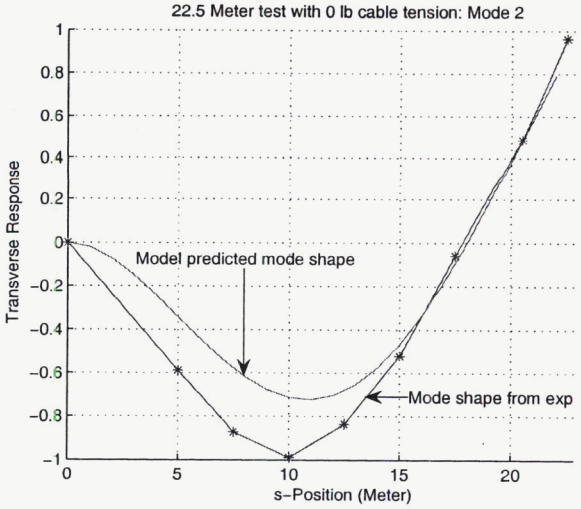

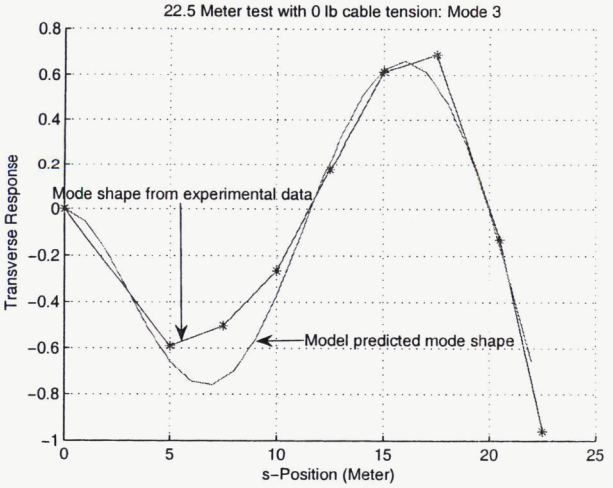

Data Analysis:
22.5 Meter test with 5 lb cable tension Mode Shape

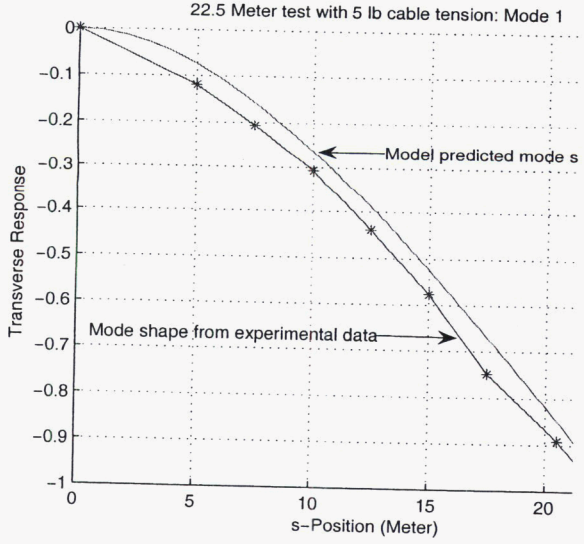

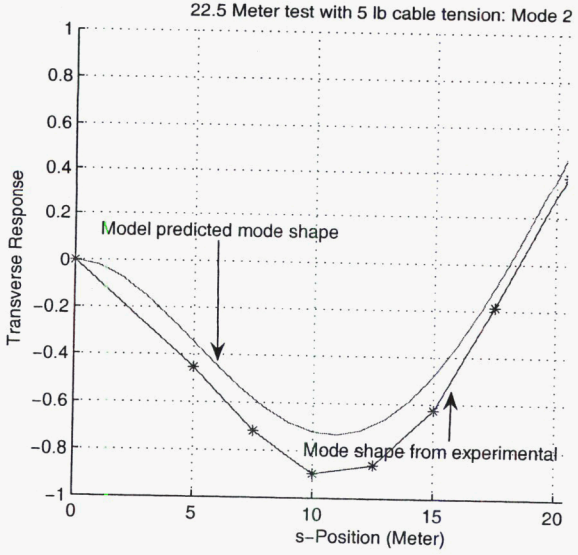

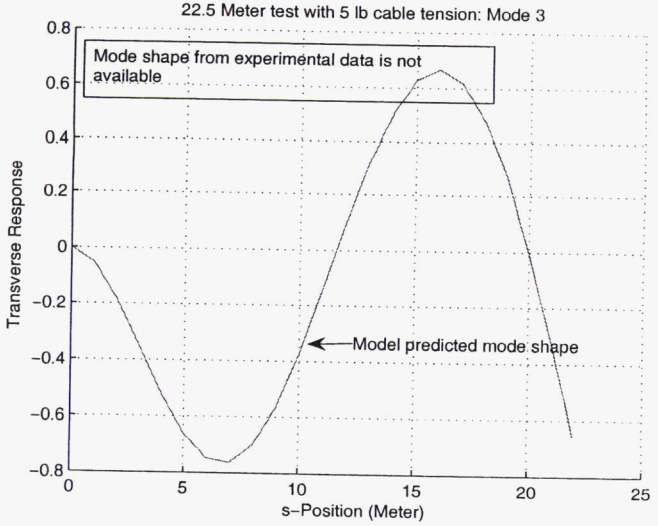

Data Analysis:
22.5 Meter test with 10 lb cable tension Mode Shape

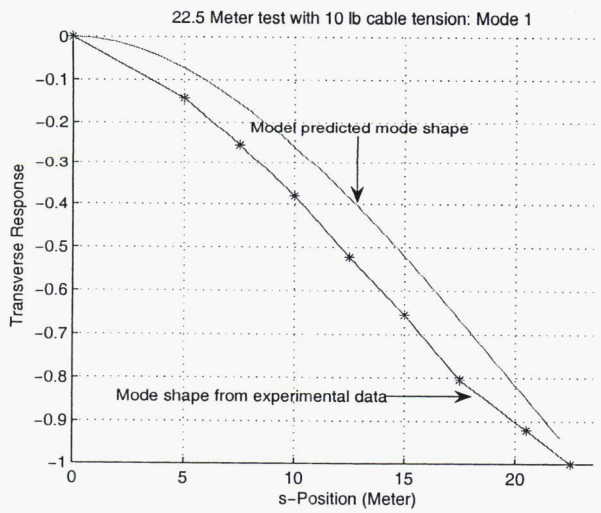

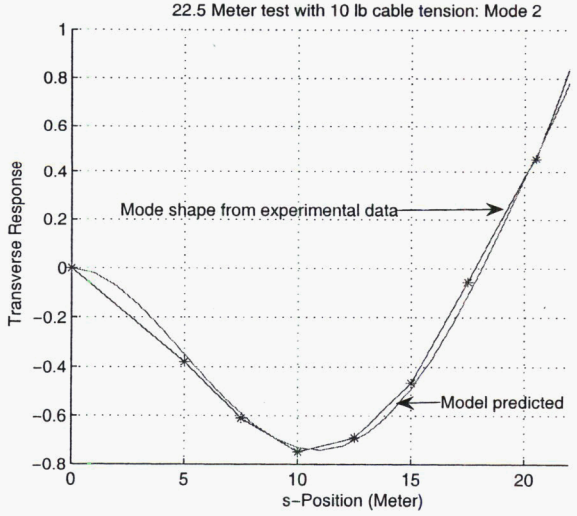

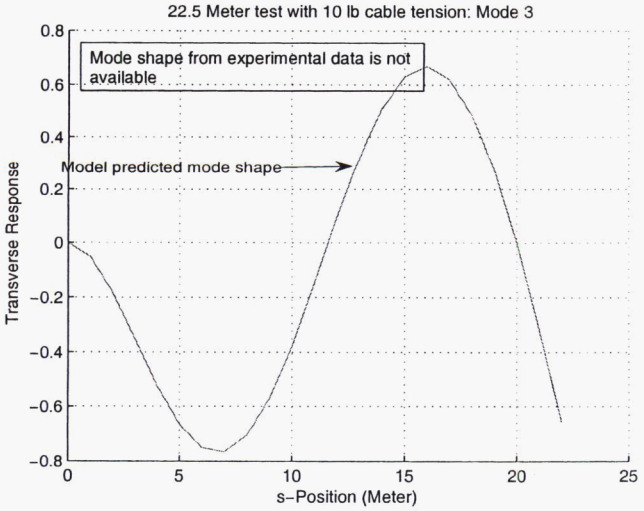

Data Analysis:
30 Meter test with 0 lb cable tension Mode Shape

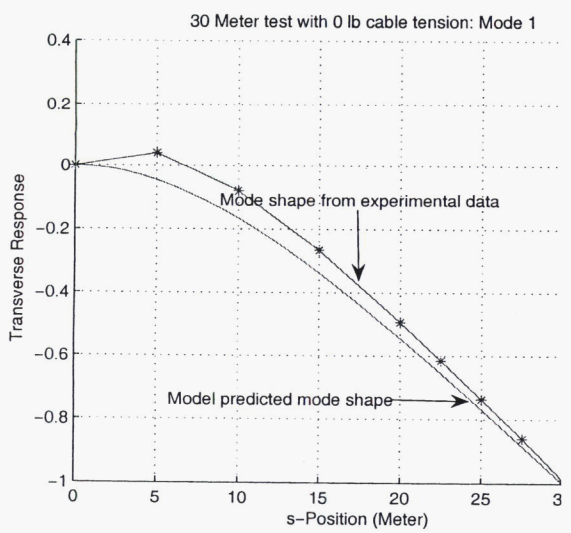

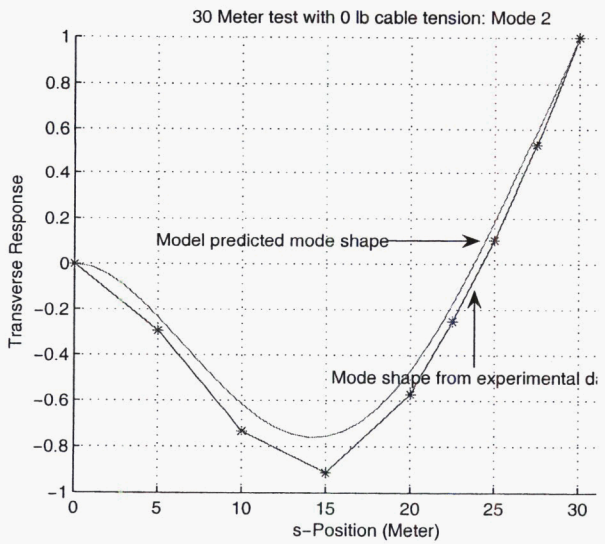

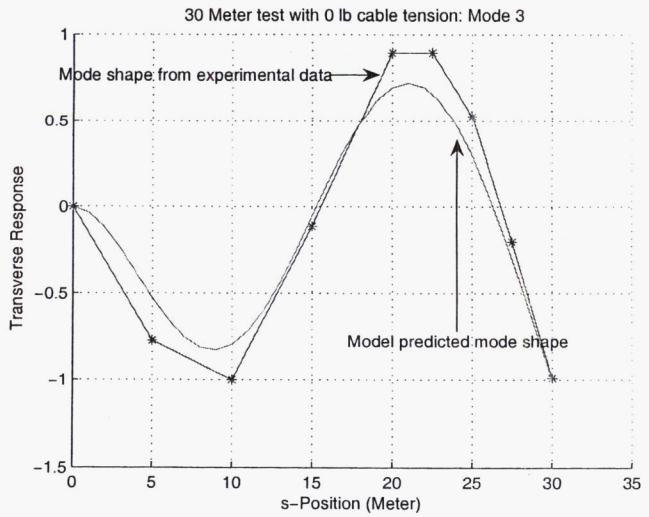

Data Analysis:
30 Meter test with 5 lb cable tension Mode Shape

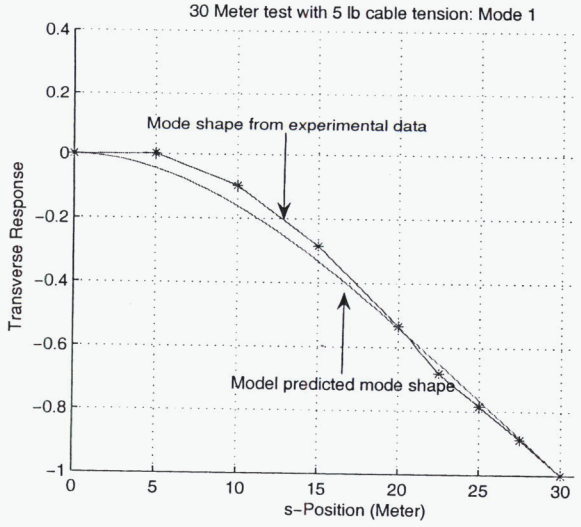

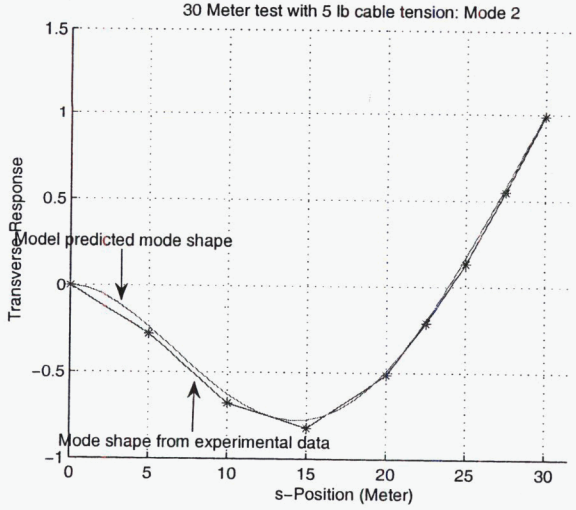

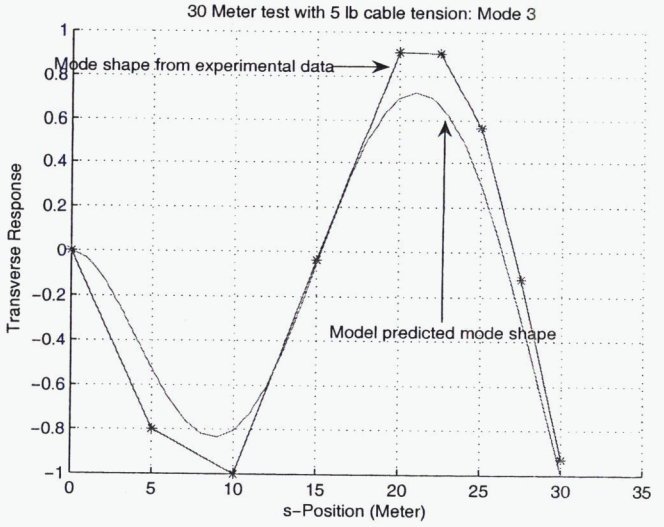

Data Analysis:
30 Meter test with 10 lb cable tension Mode Shape

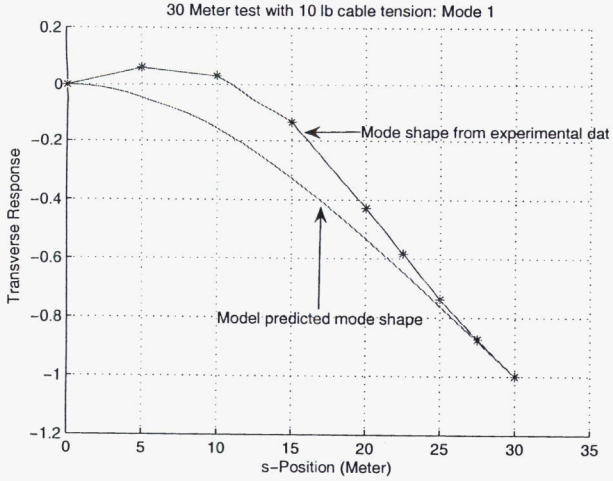

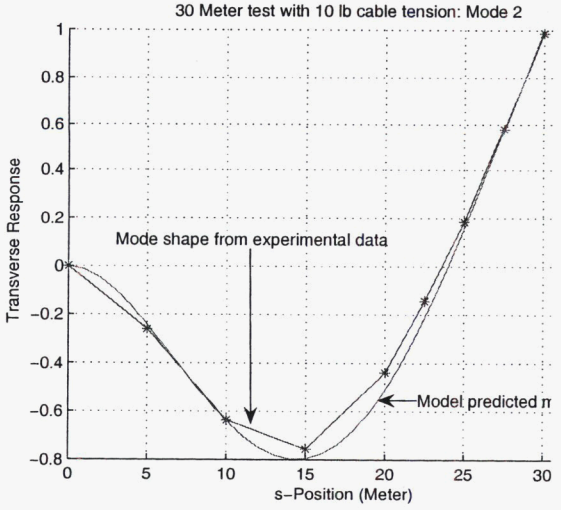

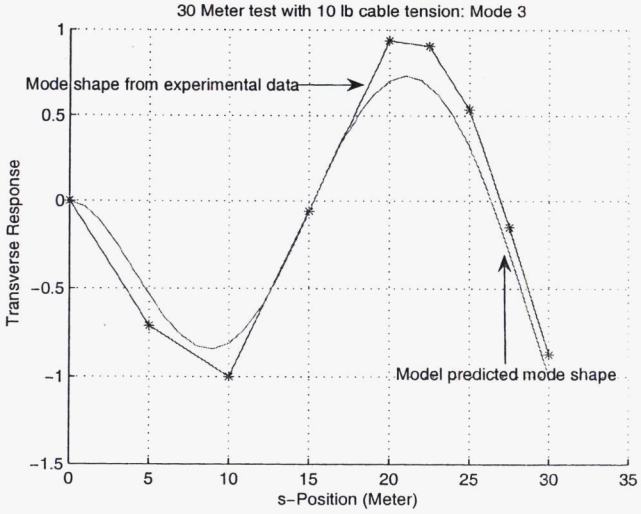

Data Analysis: Mode Shape Functions

Transverse Vibration:

- Mathematically predicted mode shapes generally agree with experiment shapes.
- Third mode shapes of some test configurations were not obtained.

Angular Vibration:

- No reliable experimental data was obtained for torsion modes:
  - Due to excessive Bending/Torsion coupling

Data Analysis:
22.5Meter test with 0, 5, 10 lb cable tension
Observing mode shape changes as axial load increases

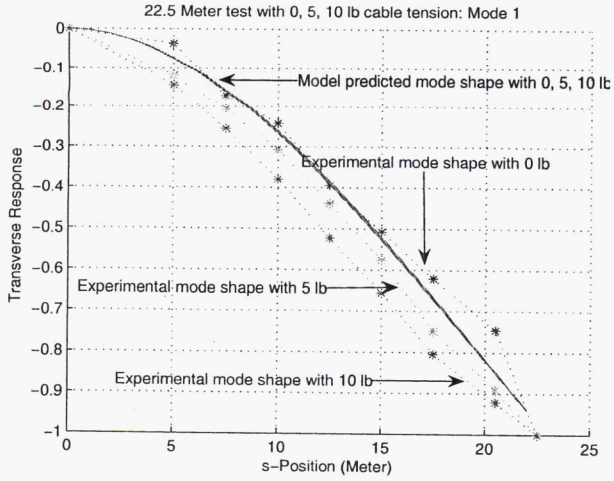

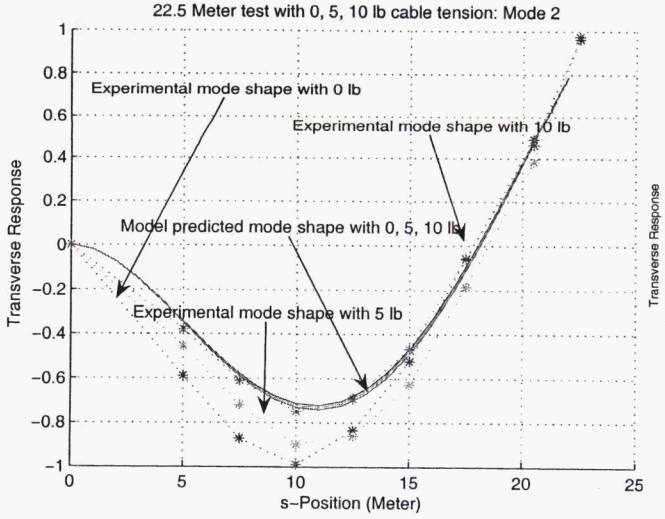

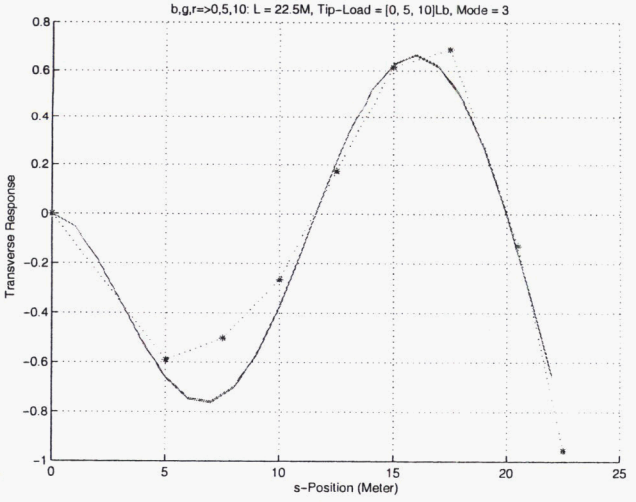

Data Analysis:

30Meter test with 0, 5, 10 lb cable tension

Observing mode shape changes as axial load increases

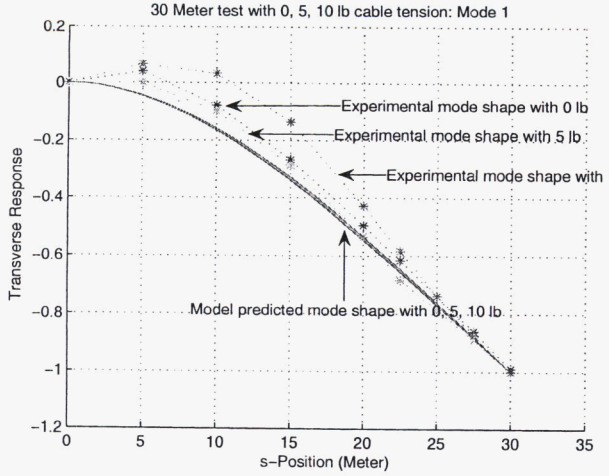

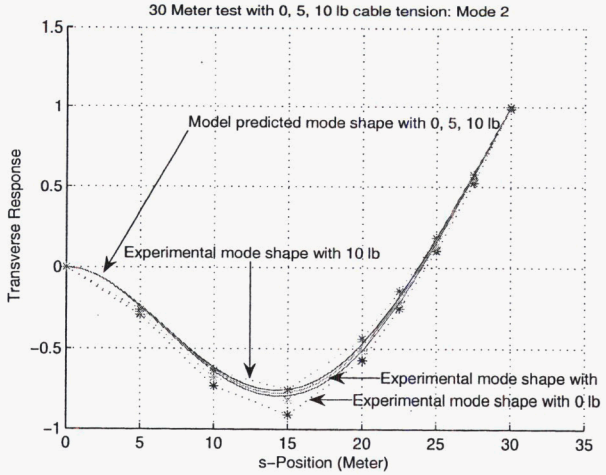

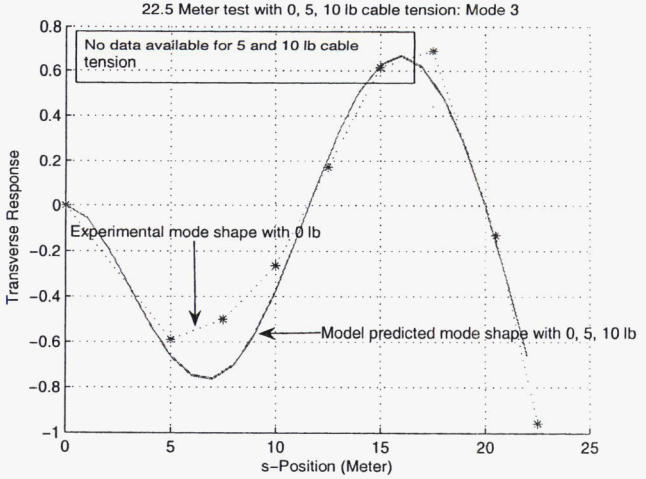

Data Analysis:
Effects of Axial Loads on Mode Shape

- In theory, mode shapes of a clamped/free beam should not change much with respect to its axial load.
- Such a phenomenon was observed in mode shapes of the mathematical model.
- However, experimental modes show significant changes with respect to axial load.

Data Analysis: Torsion FRF Analysis

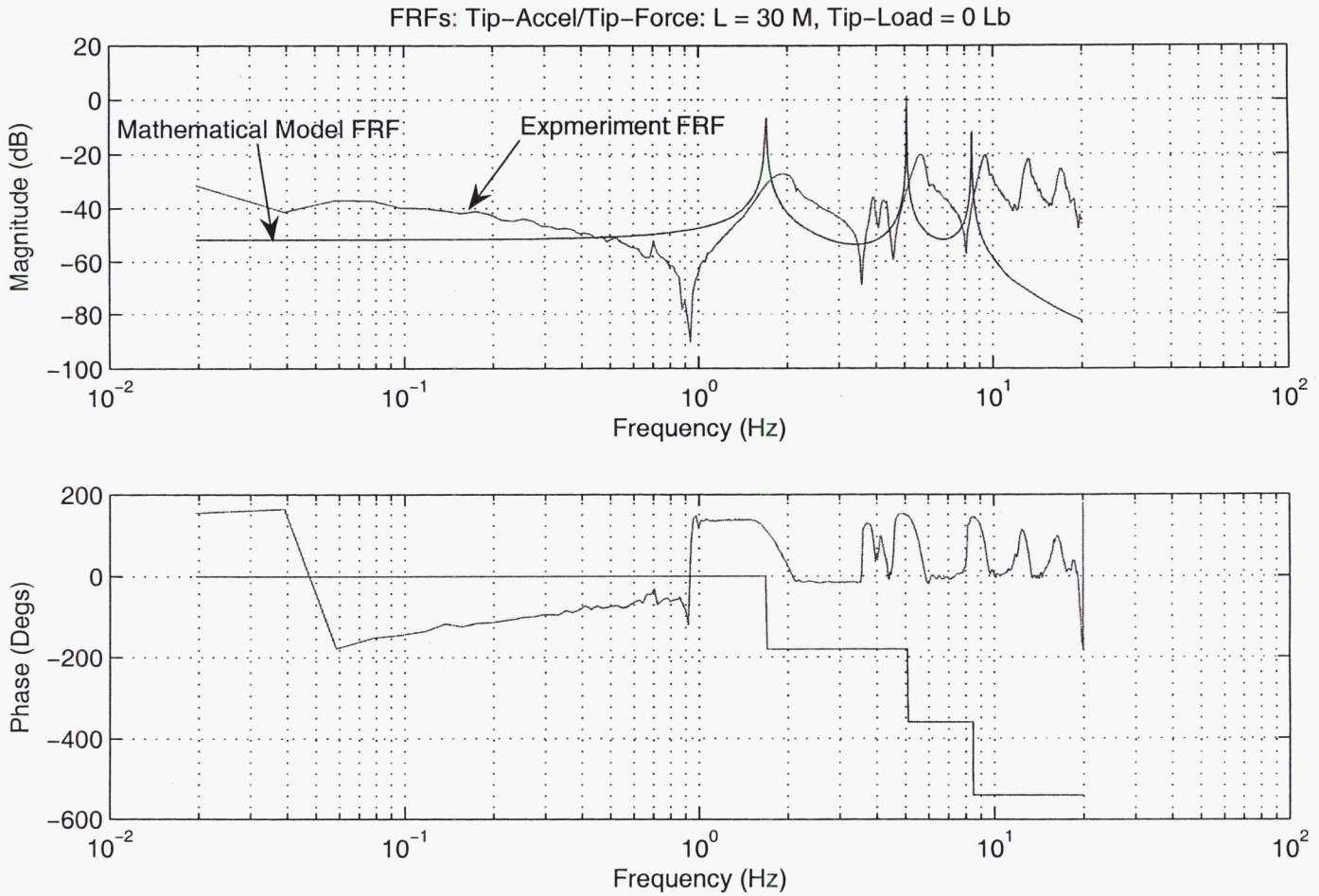

Data Analysis: Torsion Model Analysis

- No reliable experimental mode shapes available.
- Accordingly, no modal analysis of experimental data was done.
- FRF analysis shows the mathematical model is reasonable.

Concluding Remarks

- Limited angular vibration data was obtained due to coupling effects.
- Mixed results likely due to large and un-modeled angular-transverse vibration coupling. Therefore:
  - -Bow should be modeled
  - -Coupling should be modeled
- Difference between math model and experiment frequencies reduced as beam length increased.
- Math mode shapes (and natural frequencies) generally agree with experimental data
- Constant bending stiffness could not be determined.